

AFML TR-70-240

**DEVELOPMENT AND CALIBRATION
OF A MACH 1.2
RAIN EROSION TEST APPARATUS**

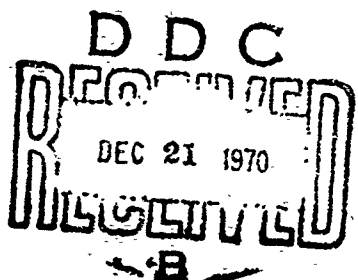
AD715909

**Charles J. Hurley
University of Dayton Research Institute**

**George F. Schmitt, Jr.
Air Force Materials Laboratory**

Technical Report AFML-TR-70-240

October 1970



This document has been approved for public release and sale; its distribution is unlimited.

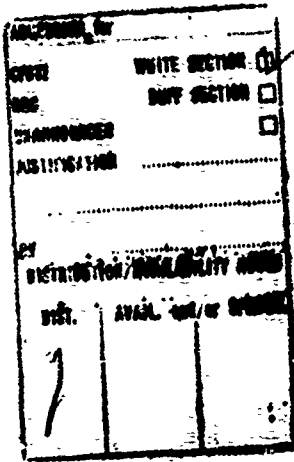
**Air Force Materials Laboratory
Air Force Systems Command
Wright-Patterson Air Force Base, Ohio**

Reproduced by
**NATIONAL TECHNICAL
INFORMATION SERVICE**
Springfield, Va. 22151

49

NOTICES

When Government drawings, specifications, or other data are used for any purpose other than in connection with a definitely related Government procurement operation, the United States Government thereby incurs no responsibility nor any obligation whatsoever; and the fact that the Government may have formulated, furnished, or in any way supplied the said drawings, specification, or other data, is not to be regarded by implication or otherwise as in any manner licensing the holder or any other person or corporation, or conveying any rights or permission to manufacture, use, or sell any patented invention that may in any way be related thereto.



This document has been approved for public release and sale; its distribution is unlimited.

Copies of this report should not be returned unless return is required by security considerations, contractual obligations, or notice on a specific document.

AFML-TR-70-240

DEVELOPMENT AND CALIBRATION
OF A MACH 1.2 RAIN EROSION
TEST APPARATUS

Charles J. Hurley
George F. Schmitt, Jr.

This document has been approved for public release and sale; its distribution is unlimited.

AFML-TR-70-240

FOREWORD

This report was prepared by the Elastomers and Coatings Branch, Nonmetallic Materials Division, Air Force Materials Laboratory. The work was initiated under Project No. 7340, "Nonmetallic and Composite Materials", Task No. 734007, "Coatings for Energy Utilization, Control and Protective Functions", and was administered under the direction of the Air Force Materials Laboratory with Mr. G. F. Schmitt, Jr. serving as project engineer. This work was accomplished in part at the University of Dayton Research Institute under USAF Contract AF33(615)-3512.

This report covers work from March 1966 to August 1969. The manuscript was released by the authors in June 1970 for publication as a technical report.

The authors gratefully acknowledge the assistance of Messrs. R. Vissoc, G. Clinehens and H. Maas in the operation of the apparatus.

This technical report has been reviewed and is approved.


WARREN P. JOHNSON, Chief
Elastomers and Coatings Branch
Nonmetallic Materials Division

ABSTRACT

Development of a Mach 1.2 Rain Erosion Test Apparatus at the Air Force Materials Laboratory, Wright-Patterson Air Force Base, Ohio, is described. This rotating arm apparatus is capable of evaluating the relative rain erosion resistance of materials and can be operated at speeds of 450 to 900 mph in a 1 or 2 inch/hour simulated rainfall. This report describes the design and development of the apparatus including the rotating arm, power train, test enclosure, rain simulation and control systems. Calibration and correlation experiments are also described.

Distribution of this abstract is unlimited.

TABLE OF CONTENTS

<u>Section</u>		<u>Page</u>
I	Introduction	1
II	Rain Erosion Test Apparatus Description	3
	1. Test Enclosure and Control Room	3
	2. Rotating Arm Apparatus and Drive System	3
	3. Rain Simulation Apparatus	4
	4. Instrumentation and Control System	5
III	Rotating Arm Power Requirements	12
IV	Rotating Arm Design	15
V	Test Specimen Design	24
VI	Test Specimen Holders	30
VII	Rainfall Simulation Apparatus Design	34
VIII	Test Enclosure and Control Room Design	38
IX	Instrumentation and Design	41
	1. Rotating Arm and Drive System Control	41
	2. Rain Simulation Control	50
	3. Closed Circuit Television Monitor and Camera	51
	4. Vibration Monitors	52
	5. Bearing Temperature Monitors	55
	6. Stroboscopic System	55
X	Calibration Experiments	58
XI	Correlation Experiments	63
XII	Discussion of Results	65
XIII	Conclusions	66
XIV	Future Work	67
XV	References	68

ILLUSTRATIONS

<u>Figure</u>	<u>Page</u>
1 AFML Rotating Arm Apparatus	6
2 Exterior View of Test Enclosure and Control Room	7
3 Double Rotating Arm	8
4 Right Angle Speed Increasing Gear Set and Pedestal Mount	9
5 Rain Ring Assembly	10
6 Control Room Instrumentation	11
7 Equivalent Diameter of Blade	18
8 Drag Coefficient of Blade	19
9 Rotating Arm Design	20
10 Sample Holder Design	21
11 Blade Cross Sections	22
12 0.0025 Airfoil Specimen Design	26
13 0.125 Radius Leading Edge Specimen Design	27
14 0.925 Radius Leading Edge Specimen Design	28
15 0.125 Radius Leading Edge Specimen Design	29
16 Specimen Holder View	31
17 Specimen Holder Schematic	32
18 Specimen Holder Cover Plate	33
19 Rain Simulation Quadrant	36
20 Hypodermic Needle Arrangement	37
21 Physical Plant Layout	40
22 Motor Drive Control Panel	44
23 Static Power Supply	45
24 Speed Increasing Gear Set	46
25 Hub and Drive Shaft	47
26 Bearing and Bearing Housing	48
27 Shaft and Bearing Housing Support Assembly	49
28 T. V. Camera and Environmental Housing	53
29 Visual Observation Method	54
30 Stroboscopic System	57

LIST OF TABLES

<u>Table</u>		<u>Page</u>
I	Operating Velocities	15
II	Rotating Arm Radius and Speed as a Function of Centrifugal Force	16
III	Physical Parameters of Double Rotating Arm	17
IV	Physical Parameters of Double Rotating Arm	23
V	Average Drop Velocities	35
VI	Rain Erosion Data (500MPH, 1 inch/hr rainfall)	59
VII	Comparison of Rotating Arm Erosion and Flight Test Erosion	64

LIST OF SYMBOLS

A = cross-section area of blade
C_D = drag coefficient
C = chord
g = acceleration of gravity, 32 ft/sec²
HP = horsepower
m = ratio of chord at blade tip to that at blade base
r = radius of blade
R = maximum radius of blade, in blade design section
S = working stress of metal in blade
t = time in seconds
V = velocity
u = velocity of gas
w = radian/second
W = weight per in³
ρ = density, Slugs/ft³
 $\bar{\rho}$ = a parameter defined by equation 10
T_w = shear stress between wall of chamber and gas
Re^N = average Reynolds number

SECTION I INTRODUCTION

The phenomenon known as rain erosion, that is, the damage to materials caused by the impingement of rain drops at high speeds, has long been a concern of the U. S. Air Force. The Air Force Materials Laboratory at Wright-Patterson Air Force Base has conducted research on rain erosion since 1947 when rain erosion was first observed on aircraft flying at speeds in excess of 400 mph.

In the course of rain erosion research over the years, the rotating arm apparatus has been found to provide the best laboratory simulation of the environment for the purposes of evaluating materials and investigation of erosion mechanisms (Reference 1). Typically, in a rotating arm apparatus, materials specimens are attached to the tip of a propeller-like blade which is rotated at a specified velocity (500 mph) through a simulated rainfall (1 inch/hour intensity). The results of rotating arm investigations have been correlated to actual flight test results both as to relative ranking of the erosion resistance of materials and the modes of failure of these materials under the influence of the droplet impingement (Reference 2). The rotating arm apparatus makes possible the attainment of velocity coupled with the random impingement of multiple drops -- all of which elements are required for proper simulation.

A variety of rotating arm apparatus have been built over the years to provide simulation for the investigation of rain erosion phenomena and these include (Reference 3):

<u>Location</u>	<u>Maximum Velocity (mph)</u>	<u>Date of Construction</u>
*Air Force Materials Laboratory Wright-Patterson AFB, Ohio	265	1944
*Cornell Aeronautical Laboratory Buffalo, New York	600	1948
Royal Aircraft Establishment Farnborough, England	600	1956
University of Cincinnati Cincinnati, Ohio	500	1955
B. F. Goodrich Company Brecksville, Ohio	600	1960
*Air Force Materials Laboratory(old) Wright-Patterson AFB, Ohio	500	1964
*Air Force Materials Laboratory(old) Wright-Patterson AFB, Ohio	1650	1958
Saab Aviation Linkoping, Sweden	750	1961
Olin Corporation New Haven, Connecticut	500	1966
Dornier Systems GmbH Immenstaad, Germany	1050	1961
Air Force Materials Laboratory(new) Wright-Patterson AFB, Ohio	900	1968
Bell Aerospace Buffalo, New York	2500	1969

The above apparatus all differ in specimen configuration and water droplet production methods but the relative rankings from each device correspond to the others. The current AFML apparatus described in this report, which is capable of velocities up to 900 mph (Mach 1.2) was developed to provide an improved capability in velocity, control of rainfall simulation and monitoring of experiments for the purpose of in-house materials development and investigation or erosion phenomena.

* No longer in existence

SECTION II

RAIN EROSION TEST APPARATUS DESCRIPTION

1. Test Enclosure and Control Room

The Mach 1.2 Rain Erosion Test Apparatus is located in Building 20-A, Area B, Wright-Patterson AFB, Ohio, which is designed specifically for propeller and rotating arm testing. Within this test building, the test enclosure and control room were constructed. The test enclosure is constructed of double reinforced, poured concrete walls with separate steel and oak bonib padding inner walls. Air vents at the base of the test enclosure insure free air movement through the enclosure and exit through the vented double roof. There are two entrances to the test enclosure: one large maintenance entrance and an entrance direct from the control room. The two entrances each contain two separate doors, each constructed of steel sheet and oak bonib padding. The design of the test enclosure insures maximum protection for operating personnel. The control room, adjacent to the test enclosure, is constructed of reinforced, poured concrete walls and roof. The entrance to the test enclosure from the control room is protected by an additional concrete curtain wall. The control room contains all the equipment and functions necessary to control and monitor the operation of the test apparatus. (See Figures 1 and 2.)

2. Rotating Arm Apparatus and Drive System

The rotating arm consists of an eight-foot diameter double arm blade. It was designed to produce high tip speeds with negative lift and a low drag coefficient. Mated test specimens are mounted at the leading edge tip sections

of the double rotating arm. The test specimens are rotated at variable speeds from 450 to 900 mph. For simulation purposes, the double arm blade is mounted horizontally on a vertical drive shaft. Power to drive the rotating arm is supplied by a high voltage D. C. power supply driving a 400 HP D. C. electric motor. The D. C. motor is coupled to a 2:1 speed increasing right angle gear drive below the double rotating arm. (See Figures 3 and 4).

3. Rain Simulation Apparatus

Simulated rainfall is produced by four curved manifold quadrants. Each manifold quadrant has twenty-four equally spaced capillaries. The capillary tubes used are specially modified hypodermic needles. Water is delivered to the four manifold quadrants simultaneously from a water storage tank located on the roof of the test enclosure. The storage tank is mounted on a vertically adjustable platform. This allows adjustment of the water head pressure by varying the height. The water level in the storage tank is maintained by an overflow standpipe. When rainfall simulation is initiated, water flows from the storage tank through low pressure solenoid valves on each manifold quadrant. Water then fills the capillaries and raindrops are produced. Drop size and drop rate are controlled by the capillary orifice diameter and head pressure of the water storage tank. The manifold quadrants are mounted above the tips of the double rotating arm. Rain drops from the simulation apparatus impact the test specimens throughout their entire annular path. The simulation apparatus can produce a wide variety of rainfall rates in the path of the moving test specimens by adjustment of the water, needle size and number but is normally run at either one or two inches per hour rainfall (See Figure 5).

4. Instrumentation and Control System

All functions of the test apparatus are controlled and monitored from the remote control room. The drive system of the double rotating arm is controlled at the operator's console. Instantaneous speed readout is monitored by an integrating digital voltmeter. Variable speed operation is possible through the operator's manual control. Pressure and temperature of the speed increasing gear drive are monitored. Dual heat sensors located on the load and axial bearing housing continuously record bearing temperatures on a recorder located in the control room. Vibration sensors are also located on the bearing housing. They measure horizontal and vertical displacement of the test apparatus on an indicator on the operator's console. A modified slave stroboscopic unit with two photo pickup sensors located on the drive shaft, and two high intensity strobe lights mounted on the test enclosure wall above and below the rotating arm provide stop motion viewing of the test specimens under actual test conditions. This function is also controlled and monitored from the operator's console. Viewing of the specimens under test is accomplished by the use of closed circuit television. A television camera in an environmental protective housing is located in the test enclosure and a television monitor is located in the control room. The operator can visually observe the erosion of the specimen undergoing evaluation. Rainfall initiation and termination is controlled also from the operator's console. Automatic timing mechanisms record the total operating time of the test apparatus, total exposure time of the specimen, and total rain simulation duration. (See Figure 6.)

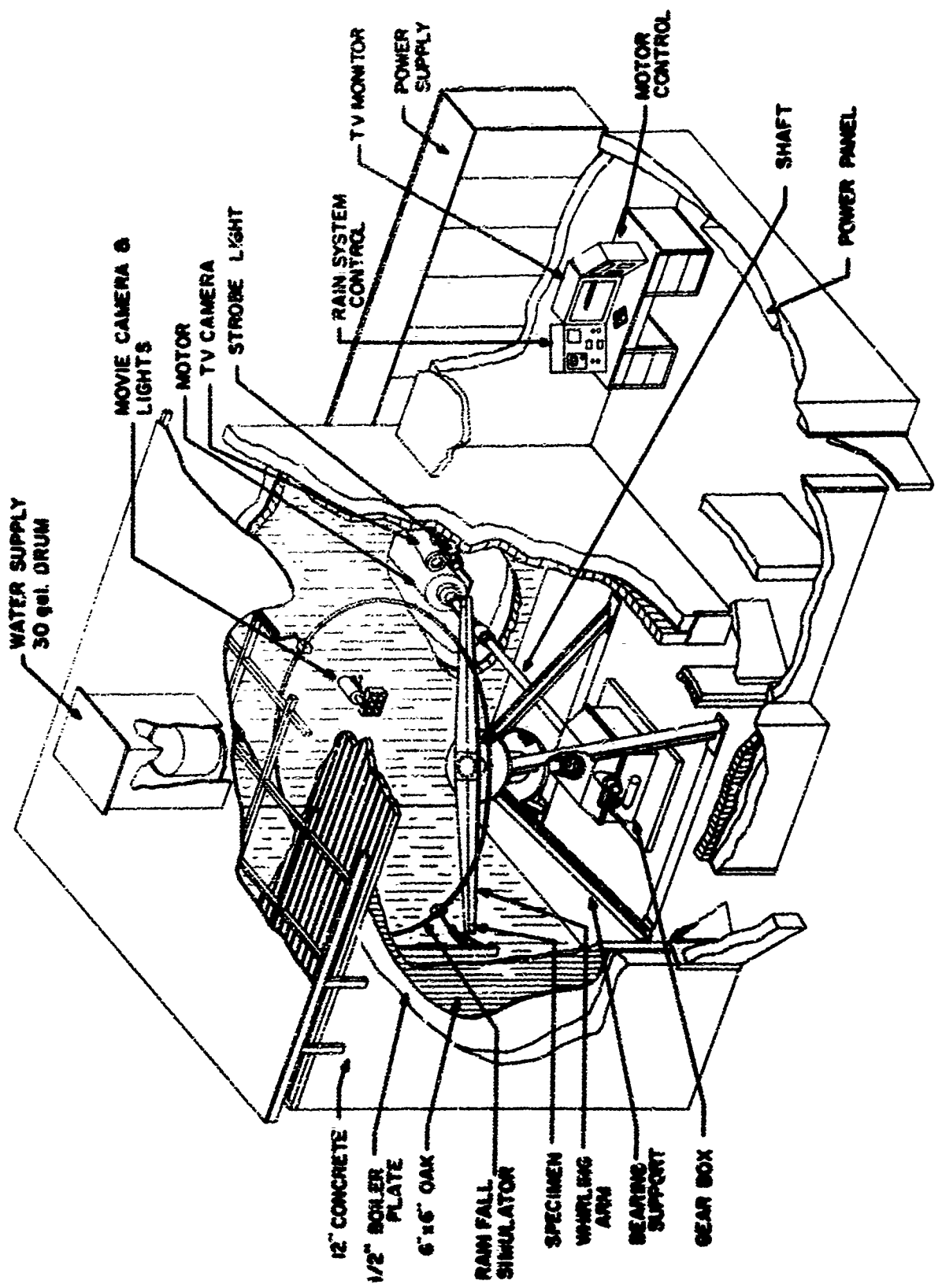


Figure 1. AFML Rotating Arm Apparatus

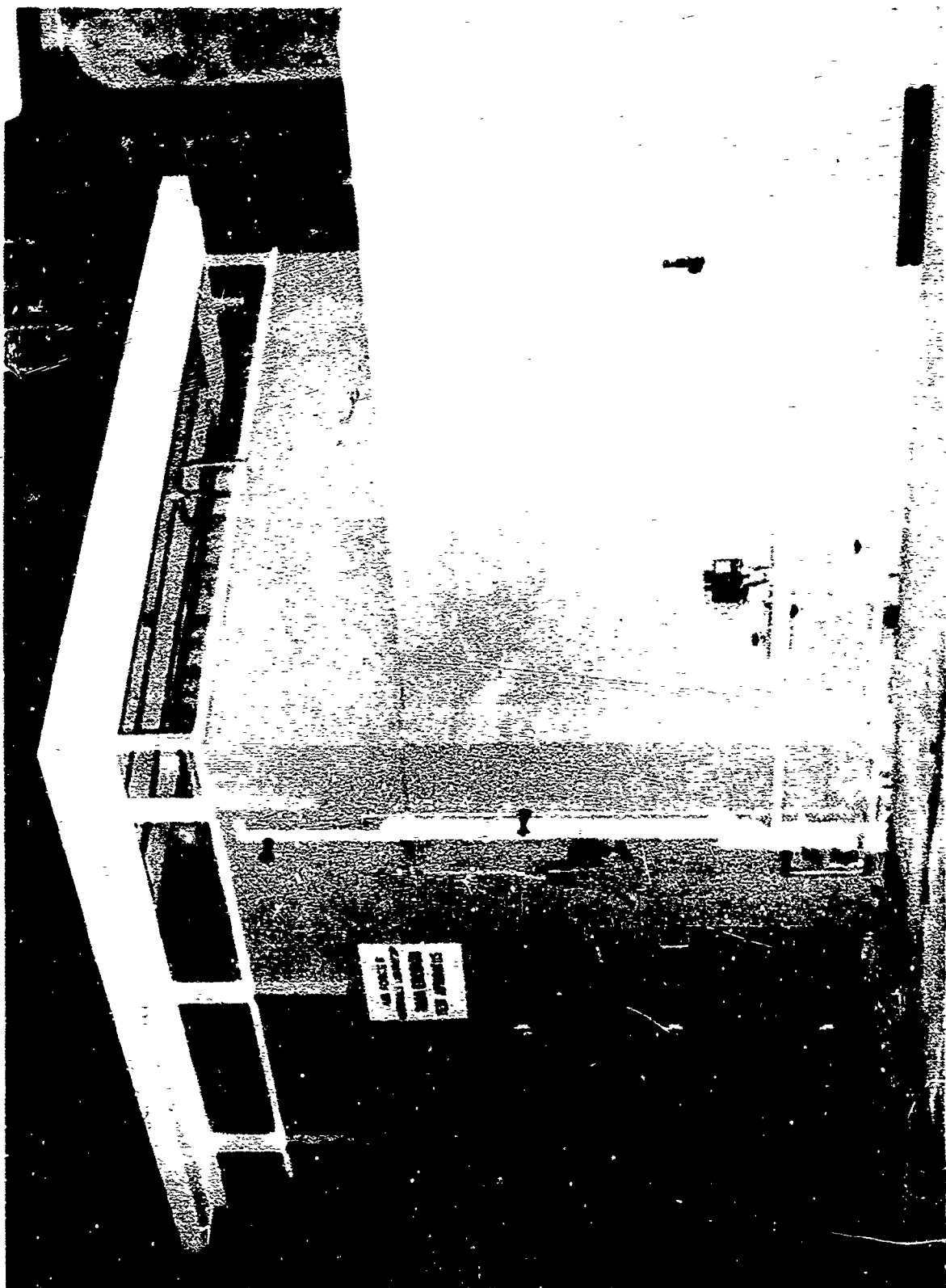


Figure 2. Exterior View of Test Enclosure and Control Room



Figure 3. Double Rotating Arm

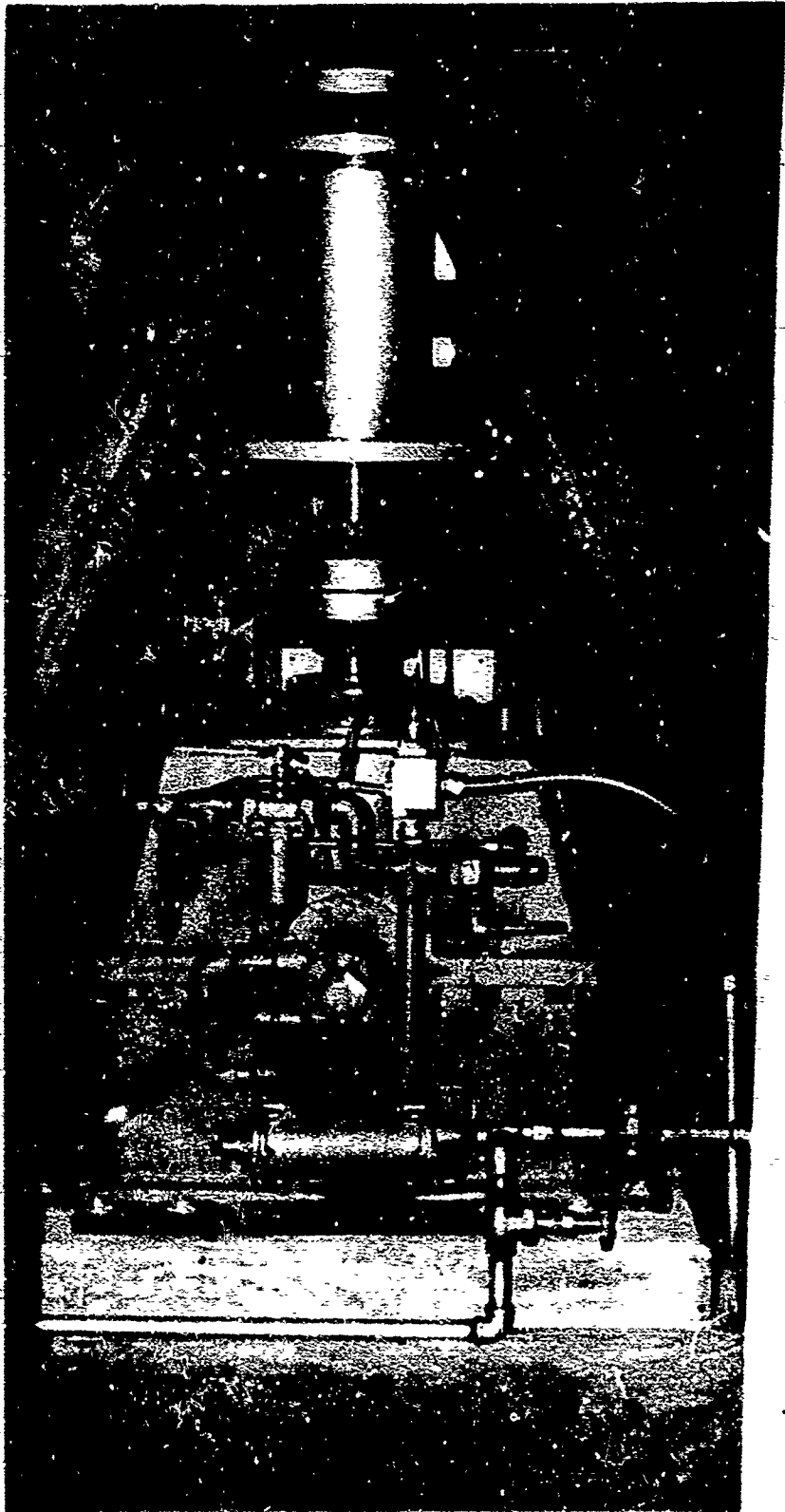


Figure 4. Right Angle Speed Increasing Gear Set and Pedestal Mount

Figure 5. Rain Ring Assembly



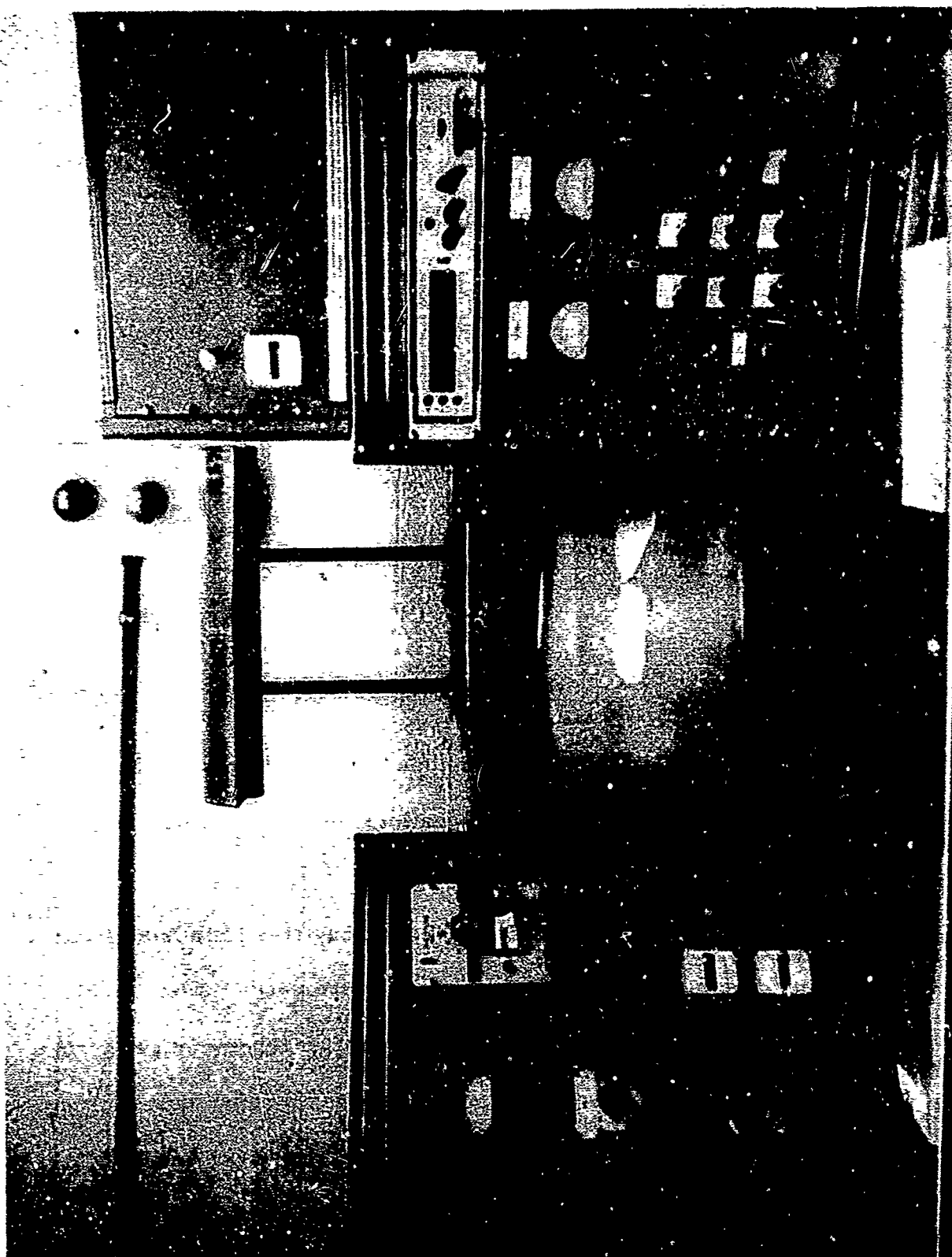


Figure 6. Control Room Instrumentation

SECTION III

ROTATING ARM POWER REQUIREMENTS

The power consumed (Reference 4) by an arm rotating through the atmosphere is a function of the amount of surface at each point along the radius. A first consideration is the manner in which the chord varies with the radius. For a design in which the stress is constant at all cross-sections (this assumes a uniform spanwise temperature) the following equation applies:

$$-SdA = \frac{12}{g} AWw^2 rdr \quad (1)$$

For a similar cross-sectional shape throughout the arm length

$$\frac{dc}{g} = \frac{6}{g} \frac{W}{S} w^2 rdr \quad (2)$$

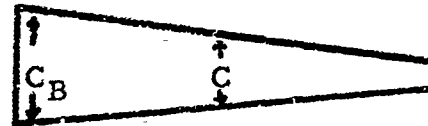
or

$$C = C_T e(V_T^2 - V^2)/4.95 (S/W) \quad (3)$$

where V is mph. For variable spanwise temperature in the blade, the allowable stress will vary and the above equations must be appropriately integrated.

It can be seen that the constant stress section deviates little from a constant taper ratio section and, for the purpose of approximate power calculations, it is assumed that the rotating arm is of constant taper geometry. In a final design computation, corrections will be needed to refine the resulting approximate value. Thus, as can be developed from the sketch below,

$$C = mC_T [1 - \frac{(m-1)}{m} \frac{r}{R}] \quad (4)$$



$$= C_T \quad m = \frac{C_T}{C_B} \quad (4 \text{ cont'd})$$

Utilizing this relation to determine the surface area, the power computations proceed as follows:

$$\text{Torque} = \int_0^R 1/2 \rho C_D V^2 c r dr \quad (5)$$

with V in ft/sec. Changing the variable from r to V

$$\text{Torque} = \frac{\rho R^2}{2V_T^2} \int_0^{V_T} C_D C V^3 dV \quad (6)$$

or

$$HP = \frac{\rho R}{(2)(550)V_T} \int_0^{V_T} C_D C V^3 dV \quad (7)$$

Substitute equation (4) for C , and, letting $V = 1100$ KM, one obtains from equation (7)

$$HP = \frac{(1.1)^2 10^6 C_T M \rho R K^3}{M_T - M_B} \int_{M_B}^{M_T} C_D [1 - \frac{M-1}{M} \frac{M}{M_R}] M^3 dM \quad (8)$$

An approximate variation of C_D with Mach number for 10% fitness ratio is as follows:

$$C_D = \begin{cases} \frac{M^2}{10} & 0 < M \leq 1 \\ \frac{1}{10M} & 1 < M \leq M_T \end{cases} \quad \left. \right\}$$

Substituting these drag coefficients into equation (8), one obtains after collecting terms

$$HP = 1.21 \times 10^5 K^3 R C_T \rho \dot{V} \quad (9)$$

where

$$\dot{V} = \left\{ \frac{M}{M_T} \right\} \left\{ M_T^3 \left[\frac{1}{3} - \frac{M-1}{4M} \right] + \frac{1}{M_T} \frac{3}{28} \frac{M-1}{M} - \frac{1}{6} \right\} \quad (10)$$

Equation (9) applies to a single blade. For a rotating arm consisting of two single blades, the power would have to be doubled.

The power requirements for a rotating arm moving at 900 mph (Mach 1.2) are derived. The horsepower required to drive a single four-foot radius blade, 10% thick, having a tip chord of 3" and a taper ratio of 7.146 in air at 1 atmosphere ($\rho = 2.378 \times 10^{-3}$ slugs/cu. ft. and a speed of sound = 1100 ft/sec) with a tip speed of 900 mph is found as follows:

$$K = \frac{1100}{1100} = 1$$

$$C_T = \frac{3}{12} = \frac{1}{4} \text{ ft}$$

$$M_T = \frac{900}{750(1)} = 1.2$$

By equation (10), $\dot{V} = 0.6787$

From equation (9)

$$\begin{aligned} HP &= 1.21 \times 10^5 (1)^3 \left(\frac{1}{4} \right) (2.378 \times 10^{-3}) (0.6787) \\ &= 196.1 \text{ HP per single arm blade} \\ &= 392.2 \text{ HP per double arm blade} \end{aligned}$$

SECTION IV

ROTATING ARM DESIGN

The double rotating arm was designed for maximum operational velocities in the test specimen exposure area of 900 mph (Mach 1.2) and a limiting centrifugal force of 27,200 lbs. The design of the double rotating arm generally takes the form of a double diamond wedge. The double arm has a diameter of 8 $\frac{1}{2}$ " and was designed to obtain velocities ranging from 400 to 900 mph at the specimen center.(2.5 inch long specimen). Table I lists the various velocities obtainable in Mach number, RPM, ft/sec and MPH at the test specimen center (2.5 inch long specimen) and blade tip:

TABLE I
OPERATING VELOCITIES

SPECIMEN CENTER				ROTATING ARM TIP			
RPM	MACH NO.	FT/SEC	MPH	RPM	MACH NO.	FT/SEC	MPH
1458	0.53	587.0	400	1458	0.56	614.0	418
1823	0.66	733.0	500	1823	0.70	767.0	523
2188	0.80	880.0	600	2188	0.84	921.0	628
2552	0.93	1027.0	700	2552	0.98	1074.0	732
2917	1.06	1173.0	800	2917	1.10	1216.0	829
3282	1.20	1320.0	900	3282	1.26	1381.0	942

The increasing rotating arm radius and rpm for speeds ranging from 400 to 900 mph as a function of centrifugal force is shown in Table II.

In the selection of materials for the double rotating arm, prime consideration was given to the strength to weight ratio, since the taper ratio

TABLE II
ROTATING ARM RADIUS AND SPEED AS A FUNCTION OF CENTRIFUGAL FORCE

	RPM	.452	1.021	1.667	2.333	3.000	3.521	3.863
500	1400	15,750	23,360	27,100	24,160	16,910	5,110	4,350
	1500	18,080	26,810	31,120	27,730	19,410	5,870	4,990
	1600	20,580	30,510	34,400	31,560	22,090	6,680	5,680
	1700	23,230	34,440	39,970	35,620	24,940	7,540	6,410
	1800	26,040	38,610	44,800	39,940	27,960	8,450	7,190
	1900	29,010	43,020	49,920	44,500	31,150	9,420	8,000
	2000	32,150	47,670	55,320	49,300	34,520	10,440	8,880
	2100	35,440	52,560	60,990	54,360	38,060	11,500	9,790
	2200	38,900	57,680	66,930	59,660	41,770	12,630	10,740
	2300	42,520	63,040	73,160	65,210	44,650	13,800	11,740
600	2400	46,300	68,640	79,660	71,000	49,700	15,030	12,780
	2500	50,230	74,480	86,430	77,041	53,930	16,310	13,870
	700	54,330	80,560	93,490	83,330	58,330	17,640	15,000
	2700	58,600	86,880	100,810	89,850	62,910	19,020	16,180
	2800	63,010	93,430	108,420	96,640	67,650	20,460	17,400
	2900	67,600	100,220	116,300	103,670	72,570	21,950	18,670
	3000	72,340	107,260	124,470	110,940	77,660	23,490	19,980
	3100	77,240	114,520	132,900	118,460	82,930	25,080	21,330
	3200	82,300	122,033	141,610	126,220	88,360	26,720	22,730
	3300	87,530	129,780	150,600	134,240	93,970	28,420	24,170
900	3400	92,910	137,760	159,870	142,500	99,750	30,170	25,660
	3500	98,460	146,000	169,400	151,000	105,700	31,970	27,190

of the rotating arm varies exponentially with this quantity, in accordance with equations similar to Section III (3). As an illustration, given in terms of equivalent circular section of a steel blade is shown in Figure 7. An approximate variation of drag coefficient with Mach number for a 10% fineness ratio is shown in Figure 8. The drawings shown in Figures 9, 10 and 11 were used for the actual fabrication of the double rotating arm.

An annealed forging of 4340 steel was selected as the material for the rotating arm. 4340 steel met the strength to weight ratio requirements and practical machining requirements. Forging dimensions were 62" x 18 1/2" x 1 3/8". Forging weight was 870 lbs. Forging hardness was 179 BHN.

Chemical analysis indicated the following alloying materials:

C	Mn	P	S	Si	Cr	Ni	Mo
0.40	0.75	0.008	0.015	0.27	0.78	1.78	0.24

An ultrasonic test was performed by the supplier before delivery. A Magna-flux PS-800, at a frequency of 2.25, by the contact method was used. No indications of voids were found when scanned in the rough forged condition. Physical parameters of the double rotating arm using 4340 steel are shown in Tables III and IV.

TABLE III
PHYSICAL PARAMETERS OF THE DOUBLE ROTATING ARM-4340 STEEL

Sec. No.	Volume (in ²)	Wt. in ³ Vol	Lb. wt. of Sec.	Section Radius (ft)	Section V(ft/sec) at 3500 rpm	Lb. C. F. at 3500 rpm
1	184.58	0.2834	52.30	0.452	165.0	97,800
2	121.15		34.33	1.021	374.4	146,500
3	86.07		24.40	1.667	610.8	169,600
4	54.82		15.54	2.333	855.3	151,200
5	29.83		8.46	3.000	1100.0	106,000
6	7.69		2.18	3.521	1291.0	32.000
7	4.21		1.19	3.863	1416.0	27,200*

*C. F. calculation includes 0.5 lb. specimen weight

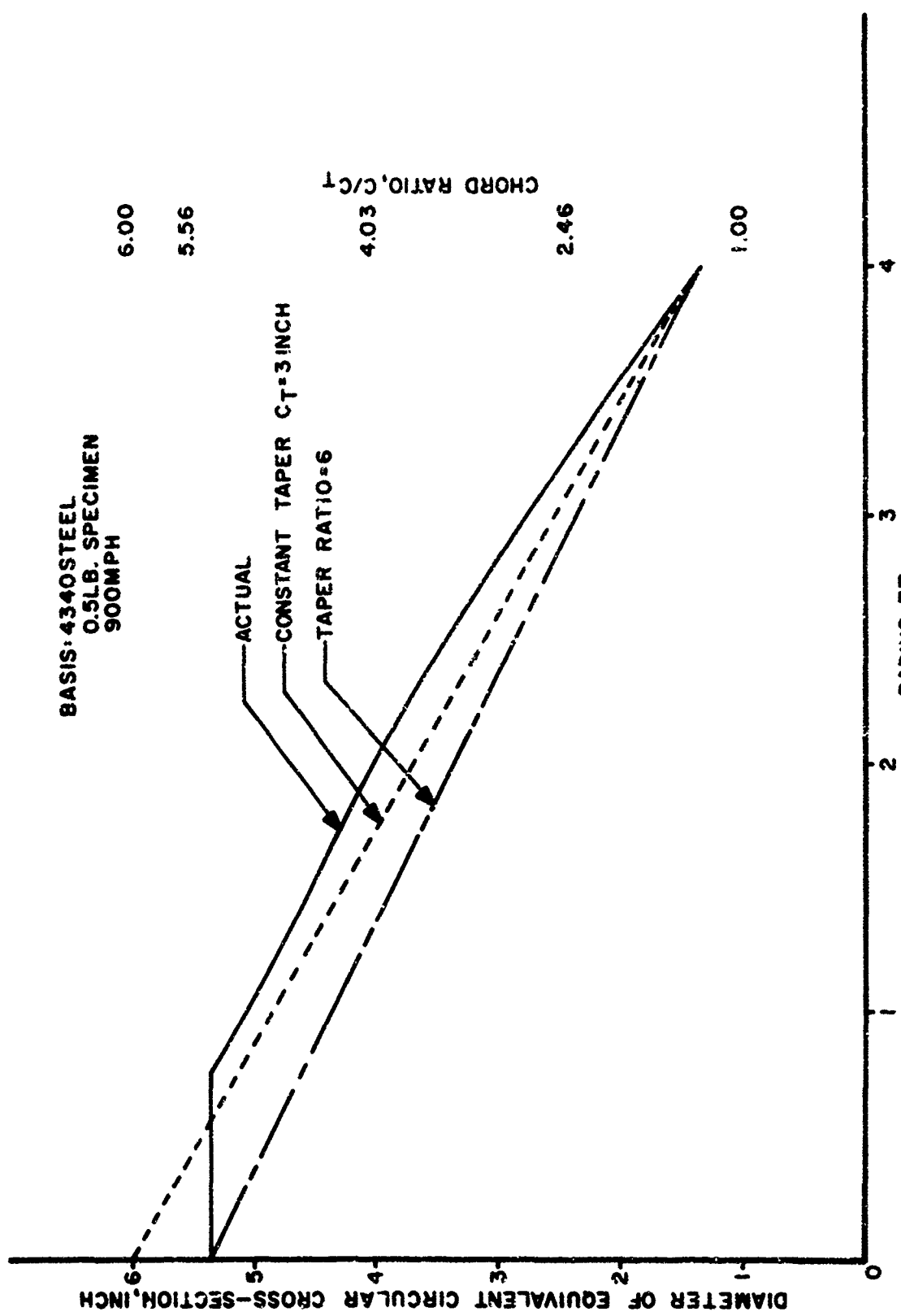


Figure 7. EQUIVALENT DIAMETER OF BLADE

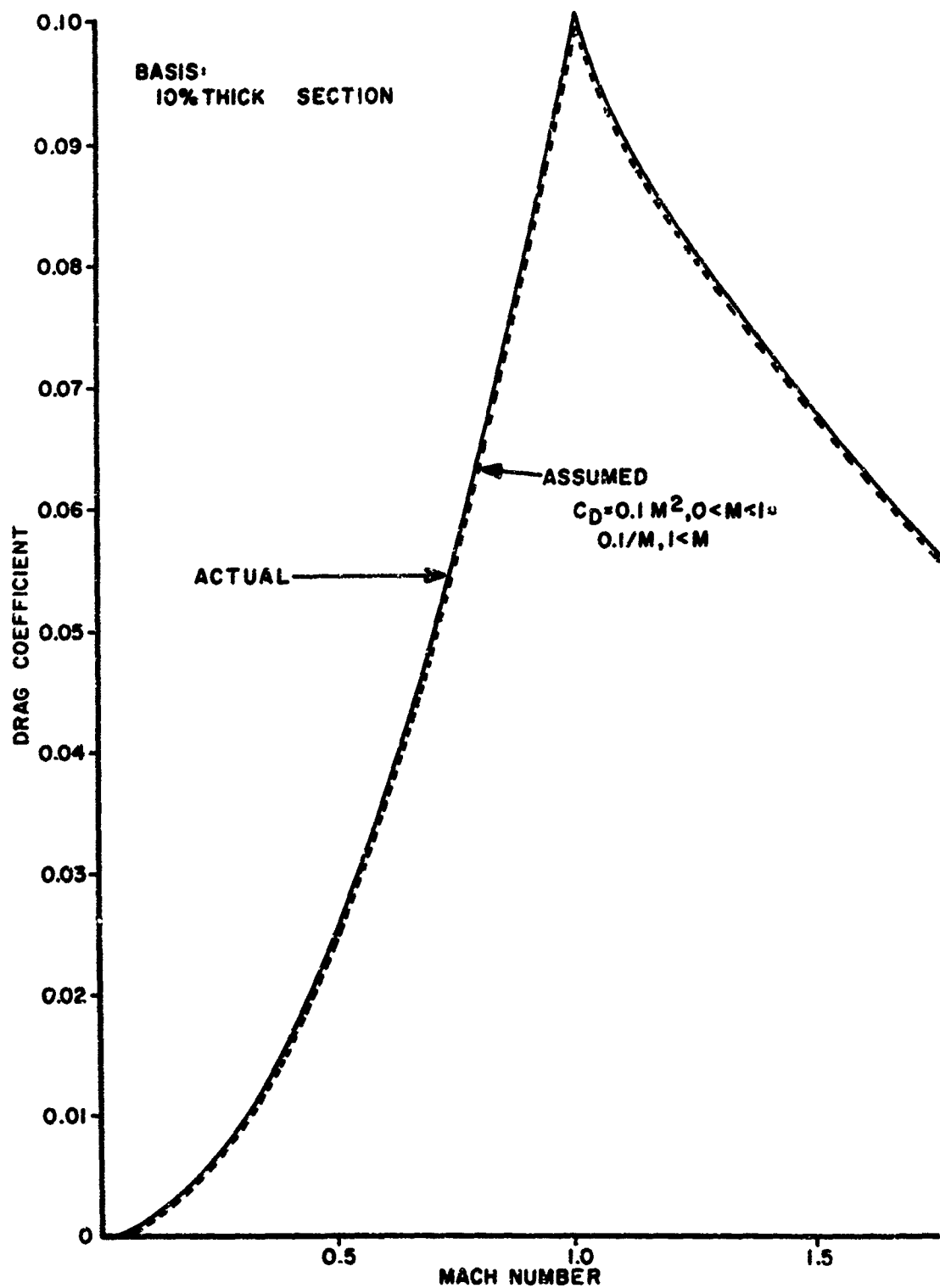


Figure 8. Drag Coefficient of Blade

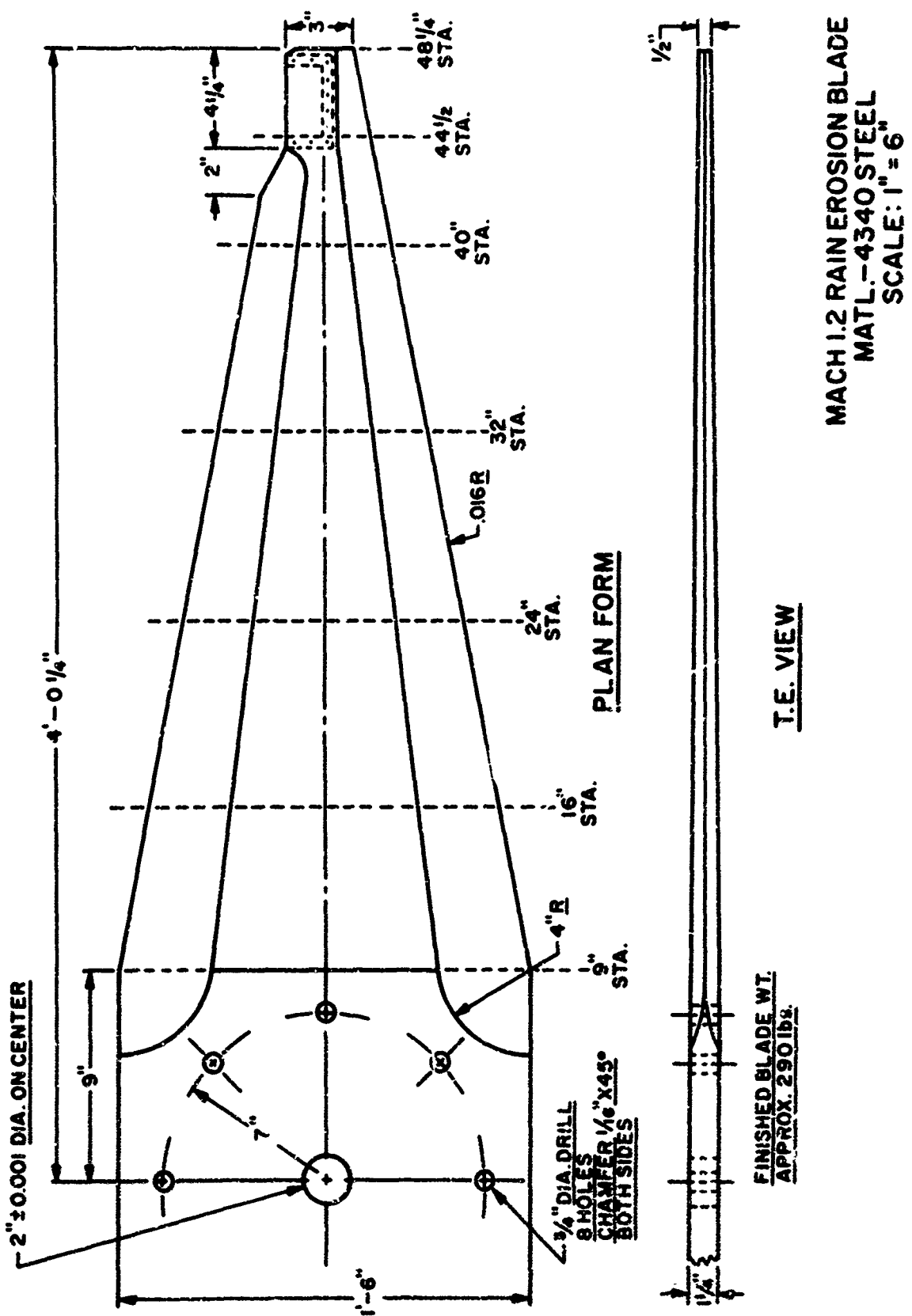


Figure 9. Rotating Arm Design

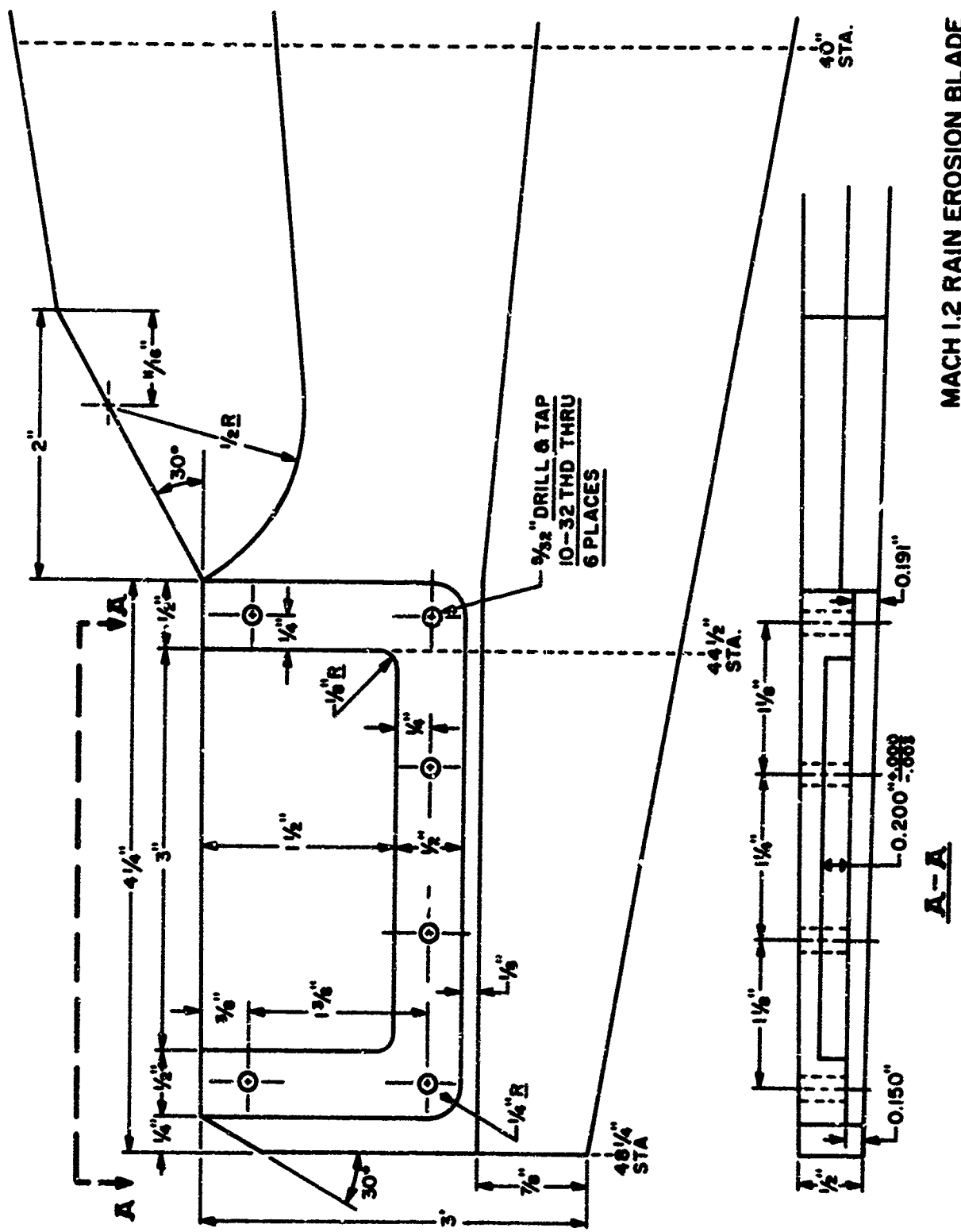


Figure 10. Sample Holder Design

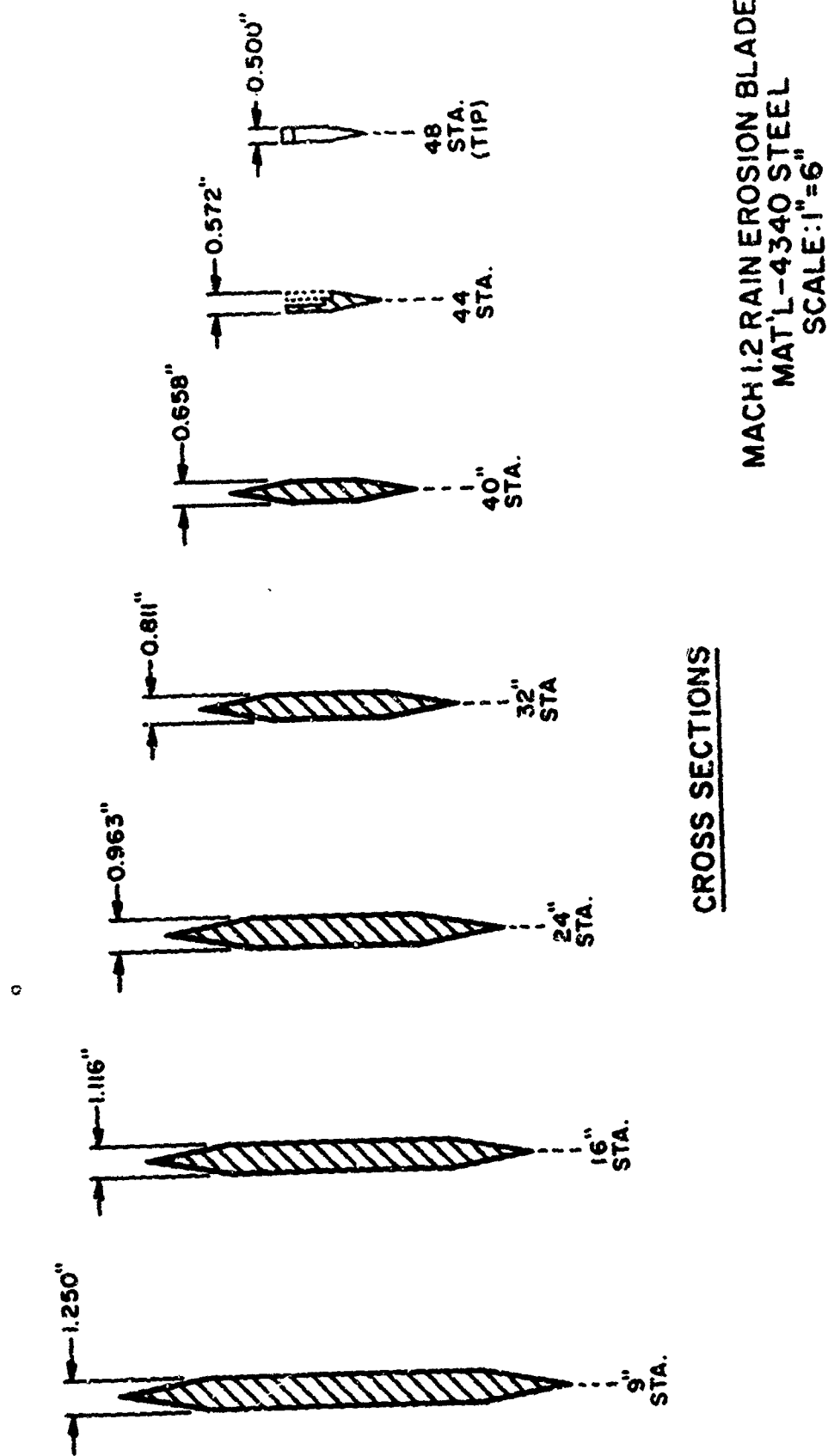


Figure 11. Blade Cross Sections

TABLE IV
PHYSICAL PARAMETERS OF THE DOUBLE ROTATING ARM-4340 STEEL

Sec. No.	Area (in ²)	Lb. C. F.	Stress, Psi
0-1	20.62	730,300	35,400
1-2	17.44	632,500	36,260
2-3	12.99	486,000	37,410
3-4	8.72	316,400	36,290
4-5	5.19	165,200	31,830
5-6	2.466	59,200	24,000
6-7	0.906	27,200	30,000

Total weight of Double Rotating Arm = 276.80 lbs.

SECTION V

TEST SPECIMEN DESIGN

The double rotating arm previously described allows attachment of two mated test specimens. This design enables simultaneous evaluation of duplicate test materials. The candidate specimens are mounted at either end of the double rotating arm and are placed such that the leading edges of the test specimens are facing the direction of travel of the rotating arm. The specimen attachment area of the rotating arm is so designed as to provide maximum versatility in test specimen configuration. Numerous test specimen configurations are possible depending upon the test apparatus limitations in maximum power capability, rotating arm stress load, rotating arm flutter and developing shock waves. The specimen shapes described below may be used as is or can be the substrate to which a candidate material is applied. Organic, inorganic, metallic and ceramic materials may be sprayed, brushed, dipped, plated, formed or bonded to the specimen substrate. Materials used in substrate fabrication may be any of the following: glass-polyester, glass-epoxy, glass-polyimide or other laminates, aluminum alloys, steels, various metals and cast ceramic or plastic materials.

Currently, five distinct specimen configurations are utilized:

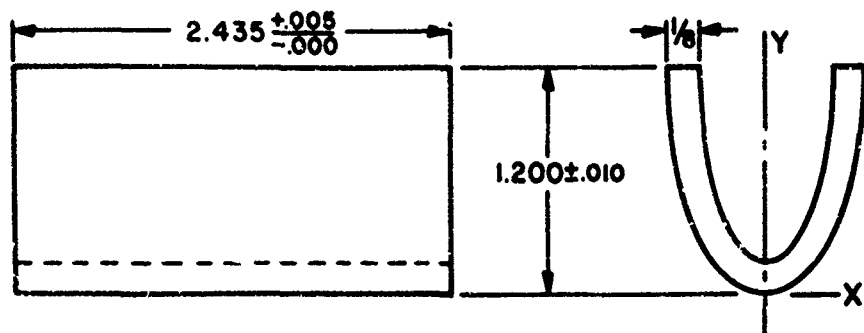
1. Cornell Leading Edge Configuration: The primary test specimen configuration was previously utilized by Cornell Aeronautical Laboratories. It is a composite design of aircraft wing leading edges (specifically an NACA .0025 airfoil). This test specimen may be fabricated from the candidate material or as the substrate for the experimental coating material. (See Figure 12.)

2. 0.125 inch Radius Leading Edge: This test specimen configuration offers a 0.125 radius leading edge over 3.937 inch length. Normally this test specimen is used as a substrate for overcoating with various experimental materials. (See Figure 13.)

3. 0.025 inch Radius Leading Edge: The test specimen described here has essentially a 4.000 inch knife edge. This specimen can be overcoated with experimental materials, but is normally used as the substrate for laminate materials bonded to the leading edge. (See Figure 14.)

4. 0.125 inch Radius Laminate Leading Edge: The laminate leading edge is usually bonded to the test specimen described in Figure 15. This specimen offers a 0.125 inch radius by a 4.000 inch length leading edge. It is normally fabricated from composite laminated experimental materials.

RAIN EROSION TEST SPECIMEN



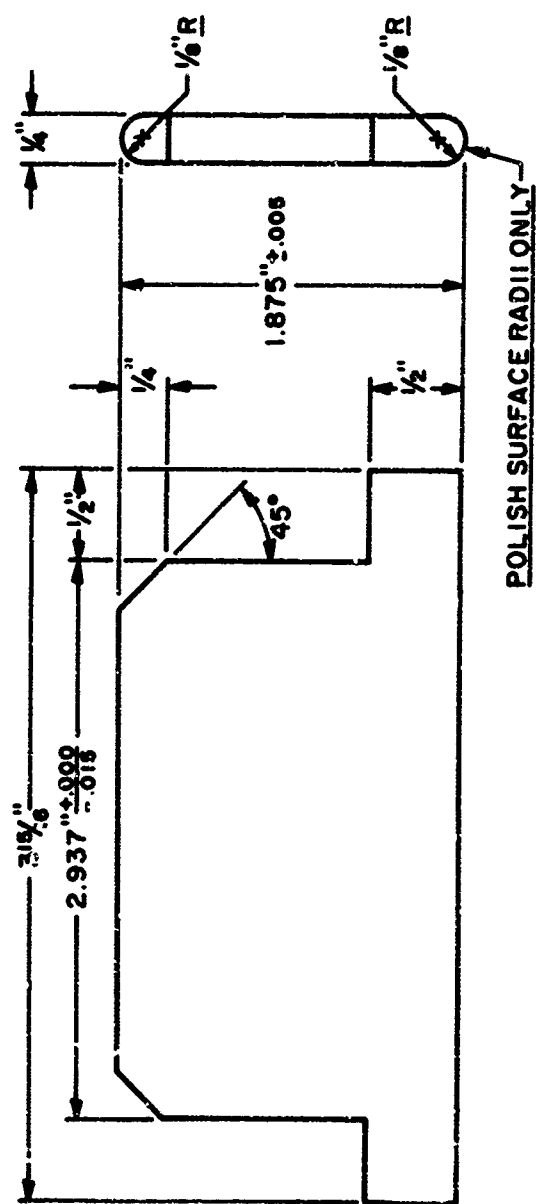
.0025 AIRFOIL-4 INCH CHORD

DISTANCE FROM LEADING EDGE

% CHORD	ORDINATE (Y)	ABSCISSA (X)
.00	.00	.000
1.25	.05	.158
2.50	.10	.218
5.00	.20	.296
7.50	.30	.350
10.00	.40	.390
15.00	.60	.446
20.00	.80	.478
25.00	1.00	.485
30.00	1.20	.500

OUTER DIMENSIONS OF $\frac{1}{8}$ INCH SPECIMEN
DIMENSIONS IN INCHES
MATERIAL - 2024-T4 ALUMINUM

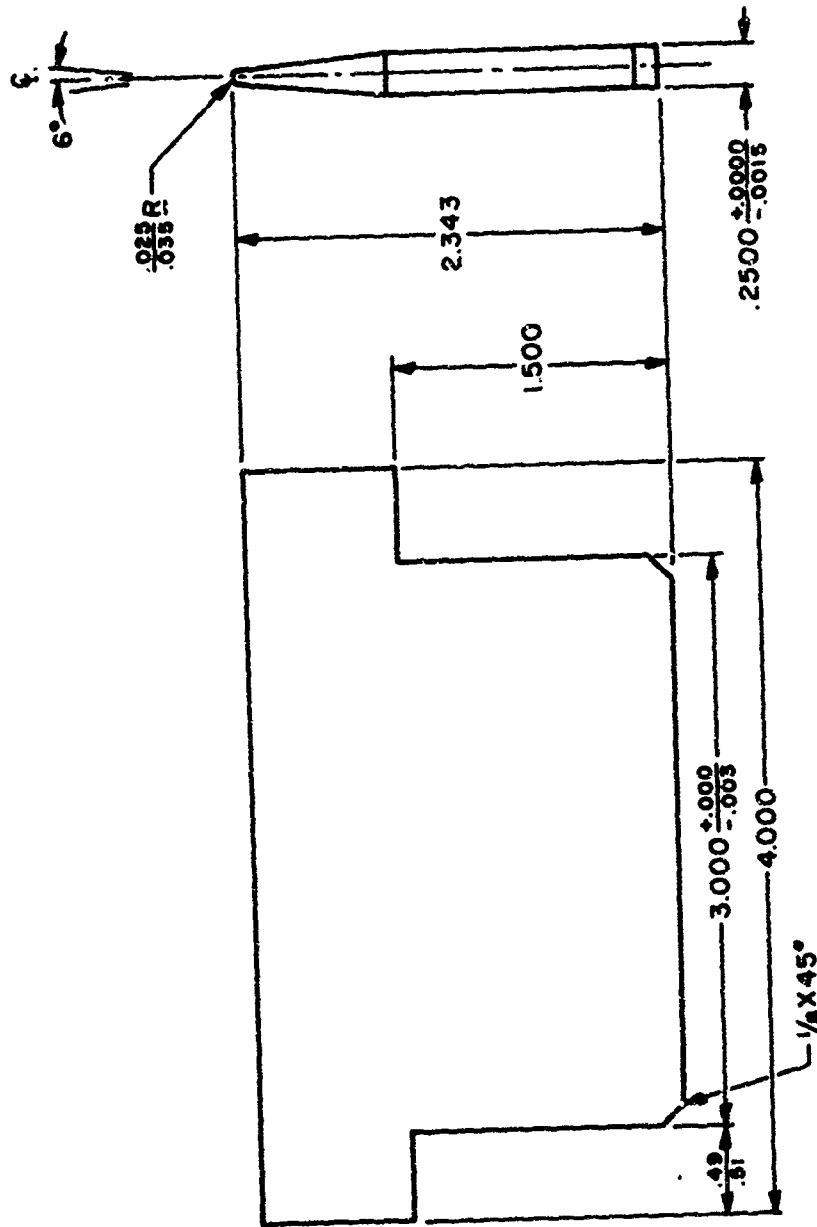
Figure 12. 0.0025 Airfoil Specimen Design



NOTE: TOLERANCE $\pm \frac{1}{16}''$ EXCEPT WHERE NOTED.
BREAK ALL SHARP EDGES

MACH 1.2 RAIN EROSION BLADE
TEST SPECIMEN
MAT'L - 2024-T4 OR 6061 ALUM.

Figure 13. 0.125 Radius Leading Edge Specimen Design



MACH 1.2 RAIN EROSION BLADE
TEST SPECIMEN
MAT'L-2024-T4 OR 6061 ALUM.

Figure 14. 0.025 Radius Leading Edge Specimen Design

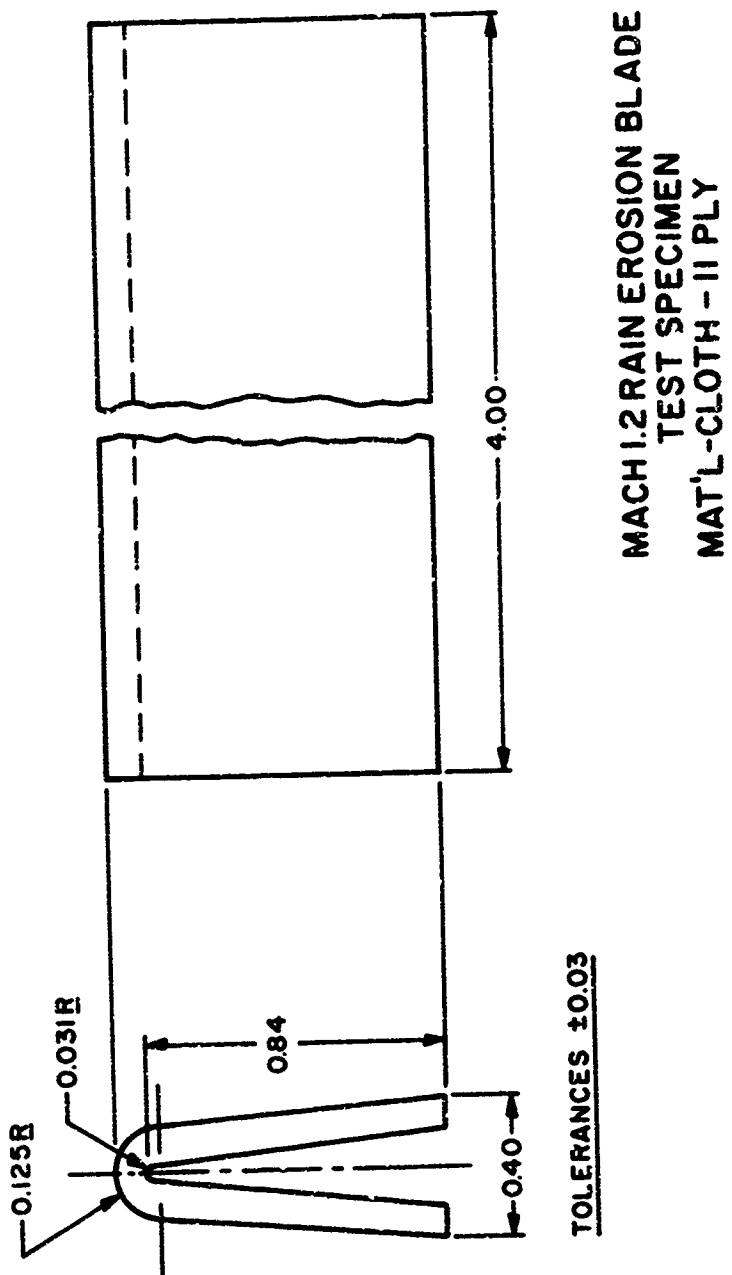


Figure 15. 0.125 Radius Leading Edge Specimen Design

SECTION VI

TEST SPECIMEN HOLDERS

Two distinct mounting holders were developed, which allow testing of the five separate specimen configurations described in the previous section. The mounting holders were designed to ease installation of test specimens and to reduce down-time between test runs. All specimens or mounting holders fit into a pocket machined into the leading edge at the outboard ends of the double rotating arm. The test specimen holder shown in Figure 16 is designed for the Cornell leading edge configuration described in No. 1 of Section V. Schematic drawing is shown in Figure 17. The cover plate holder described in Figure 18 is used to mount specimen configurations No. 2, 3, 4, and 5 in Section V. The pocket arrangement of the double whirling arm permits design of various specimen shapes and specimen holders as future testing requirements change.

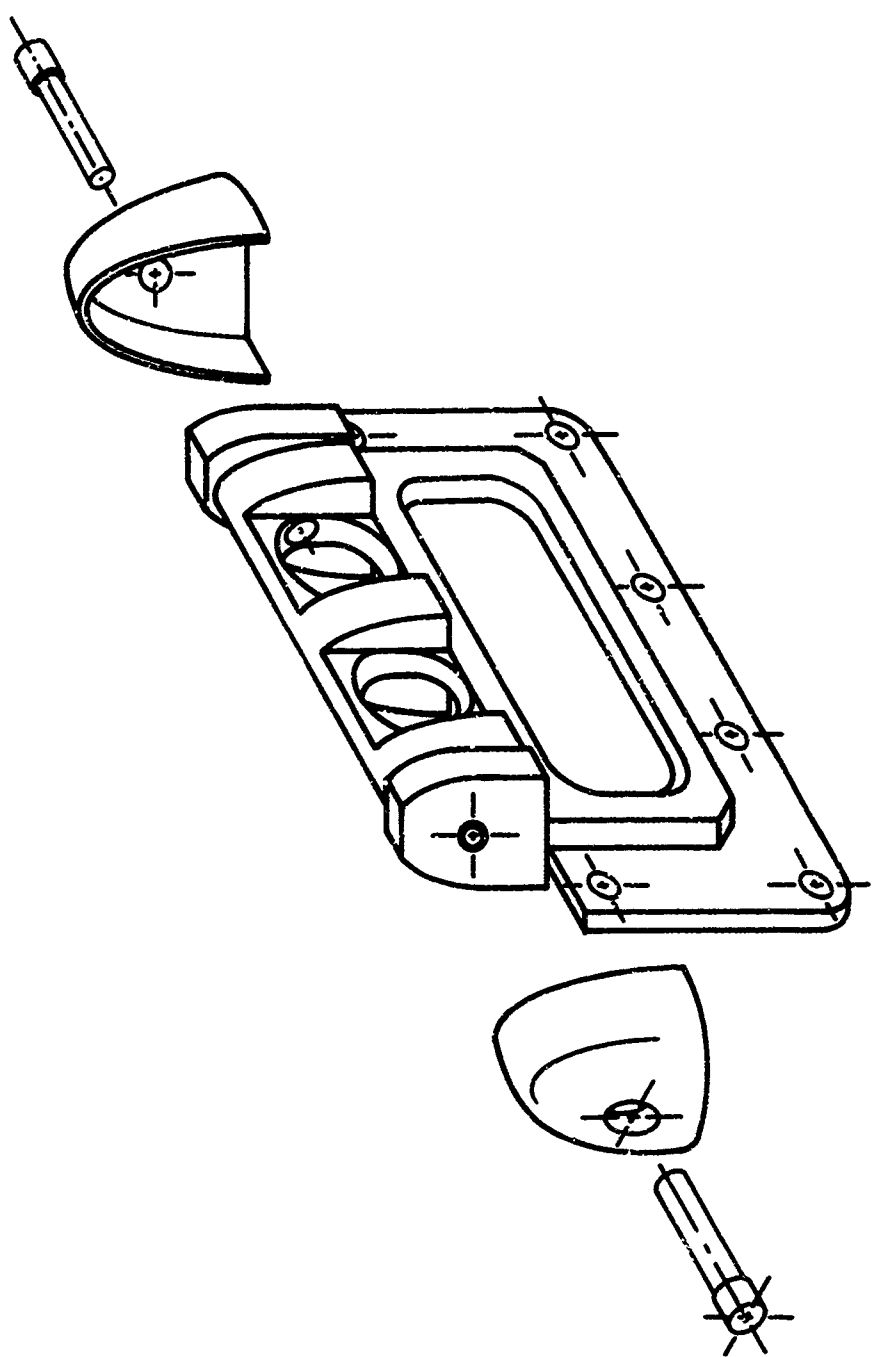


Figure 16. Specimen Holder View

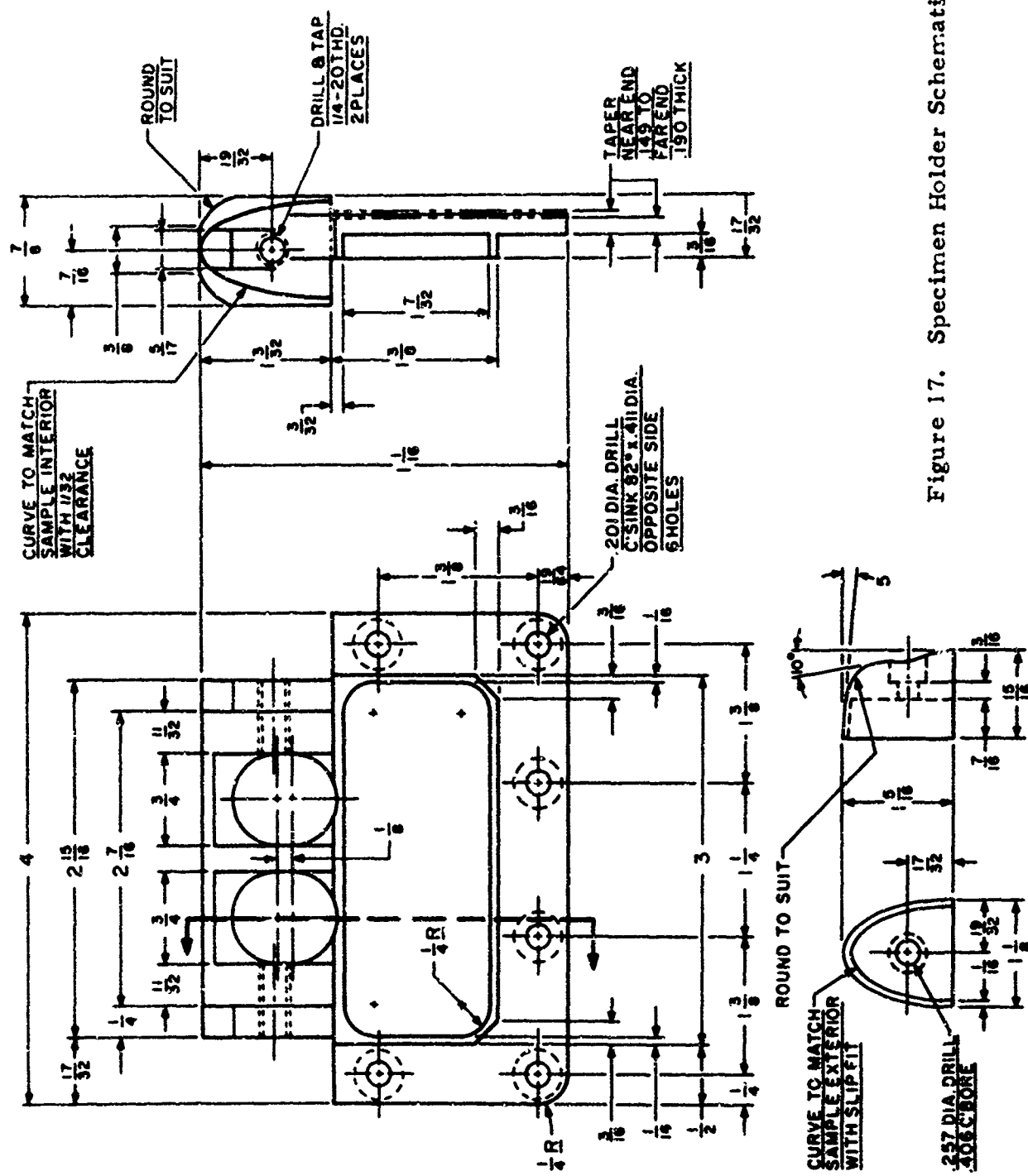


Figure 17. Specimen Holder Schematic

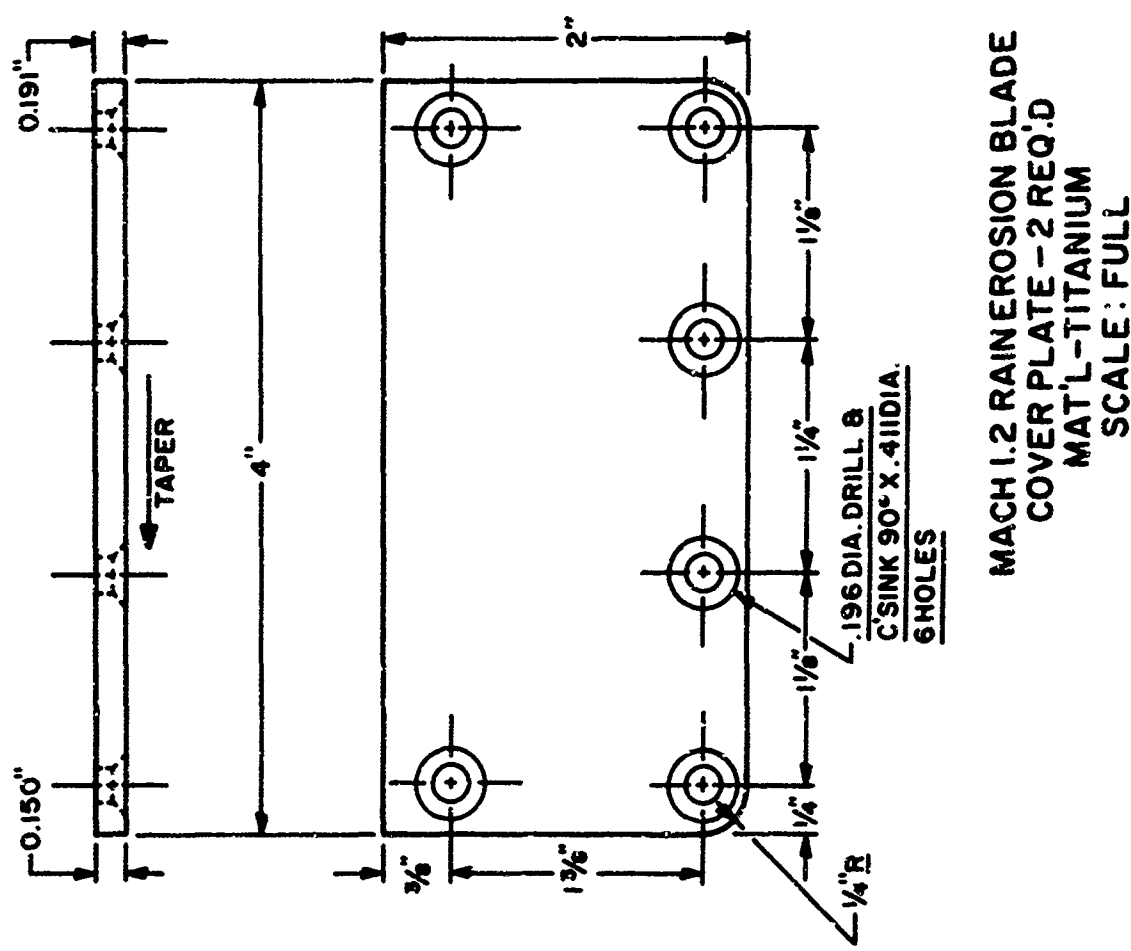


Figure 18. Specimen Holder Cover Plate

SECTION VII

RAINFALL SIMULATION APPARATUS DESIGN

Water for the rainfall simulation apparatus is piped to the control room. At this site, the water flow is controlled and passed through a filtering system. Filtration is accomplished by passing the water through a 5 micron wound cotton fiber filter and through a 0.5 micron porous stainless steel filter. Water is then piped to a 32 gallon reservoir tank located on top of the test enclosure. The reservoir tank is equipped with an overflow stand pipe and a solenoid operated dumping valve. The tank is mounted on a platform which can be raised and lowered vertically to control the head pressure of the water delivered to the rainfall simulation manifolds. Water is delivered to the quadrants through copper lines to each manifold of the rainfall simulation apparatus. Four separate solenoid valves control the water flow to each quadrant. The solenoid valves are mounted directly behind the quadrants and insure instantaneous initiation and termination of the simulated rainfall. Water is passed through the solenoid valves into the four curved manifolds mounted horizontally above the double rotating arm. (See Figure 19). Water passes from the manifolds through vertically mounted capillary tubes (modified hypodermic needles) in the form of water droplets. The drop size and drop rate are controlled by the capillary interior diameter and tube length with an appropriate head height pressure. The height of the manifolds can be varied to produce a desired drop velocity. The manifolds can be moved horizontally toward the center of the test enclosure over the

double rotating arm to compensate for centrifugal pumping effects caused by high speed operation of the rotating arm.

Due to the high concentration of soluble salts in the water, it was necessary to install a nitrogen gas purging system. During shutdown periods, residual water in the manifolds evaporated through the capillary tubes leaving salt deposits. These deposits caused malfunctions of the capillaries. The gas purging system expels the residual water in the quadrants at the end of each day's operation.

Ninety-six 27 ga (0.20 mm I. D.) capillaries mounted in the manifolds (3.03" apart) produced a continuous simulated rainfall in the annular path of the moving test specimens (See Figure 20). The manifolds can be moved vertically over a distance of five feet to produce a desired drop velocity (See Table V).

TABLE V
AVERAGE DROP VELOCITIES

Acceleration ft/sec ²	Distance (ft.)	Time (sec)	Initial Velocity (ft/sec)	Final Velocity (ft/sec)
32.2	0.5	0.175	0	5.65
32.2	1.0	0.248	0	8.00
32.2	1.5	0.306	0	9.97
32.2	2.0	0.351	0	11.31
32.2	2.5	0.393	0	12.68
32.2	3.0	0.431	0	13.89
32.2	3.5	0.465	0	15.00
32.2	4.0	0.497	0	16.03
32.2	4.5	0.527	0	17.00
32.2	5.0	0.557	0	17.94

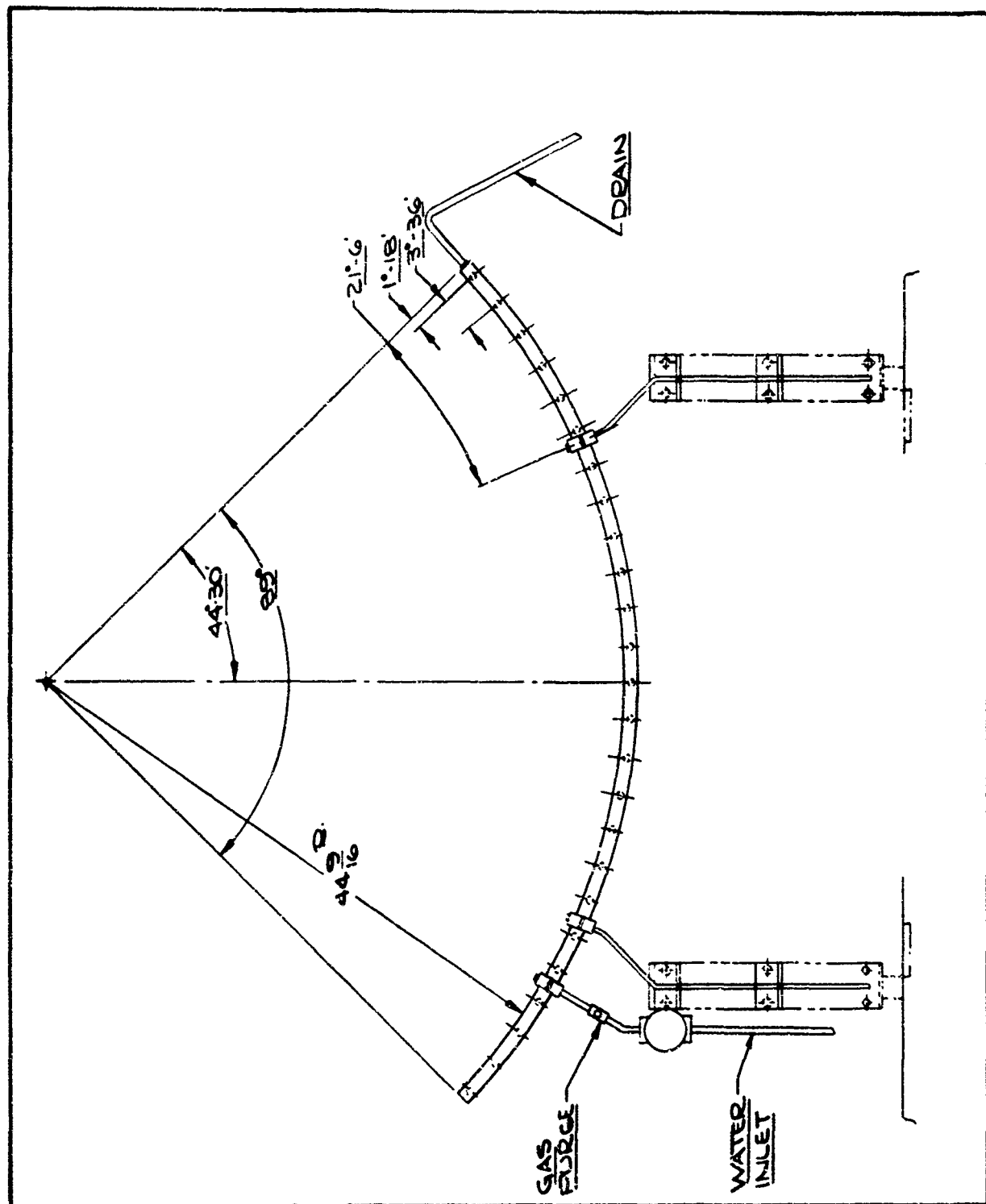
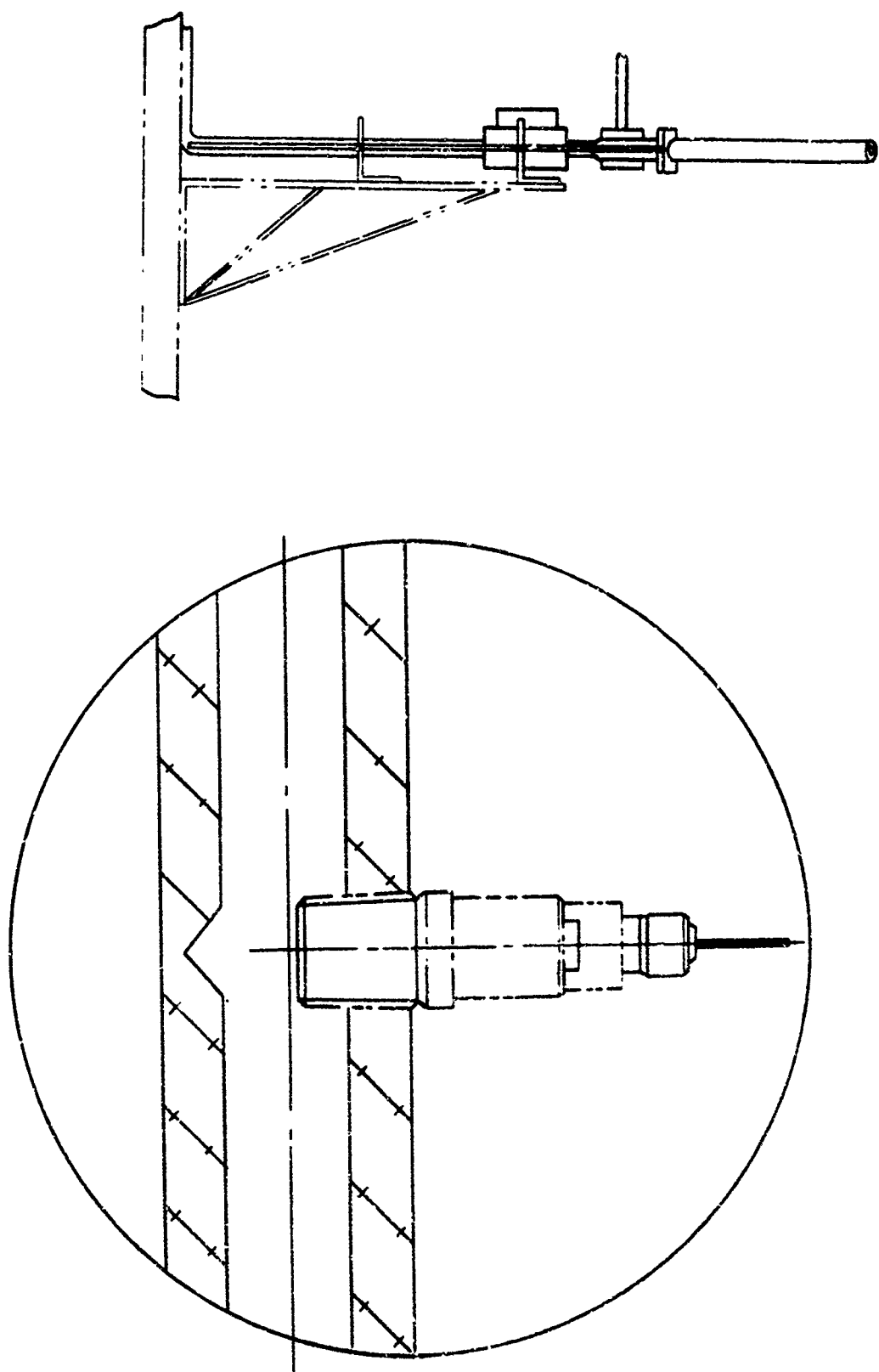


Figure 19. Rain Simulation Quadrant

Figure 20. Hypodermic Needle Arrangement



SECTION VII

TEST ENCLOSURE AND CONTROL ROOM DESIGN

The design of the test enclosure and control room incorporates the concepts of increased testing capability, maximum safety and operational efficiency. The test apparatus is located in a building designed specifically for propeller and rotating arm testing. Visible and audio warning systems, as well as, restricted personnel access have long been a part of this test site's standing orders. Approximately 600 sq. ft. of this testing site had been allocated for the construction of the rain erosion test apparatus. Construction of the test enclosure and control room required maximum protection from internal system failures and external testing operations in the vicinity of the test apparatus.

The test enclosure (14' x 14' x 12') is constructed of 12" steel-reinforced concrete, 1/2" steel, and 6" x 6" oak bomb padding. The floor is constructed of 6" reinforced concrete with a 5" raised concrete pedestal in the center. Six air vents are located in the base of the walls to provide air circulation. The bomb padding encloses the chamber on top (spaced at 2" intervals for venting) a separate roof then covers the entire enclosure. An access aperture is located in the rear wall for the connecting shaft between the motor and gear box. The test enclosure contains two entrances, one for direct access from the control room and one exterior entrance for maintenance operations. The two entrances are constructed of one inner and one outer heavy steel and bomb padding doors set in steel frames (See Figure 21).

The control room adjacent to the test enclosure (14' x 14' x 8') is

constructed of 8" reinforced concrete walls and roof. An 8" reinforced concrete curtain wall provides additional protection. All electrical power for the operation of the test apparatus is controlled from this site.

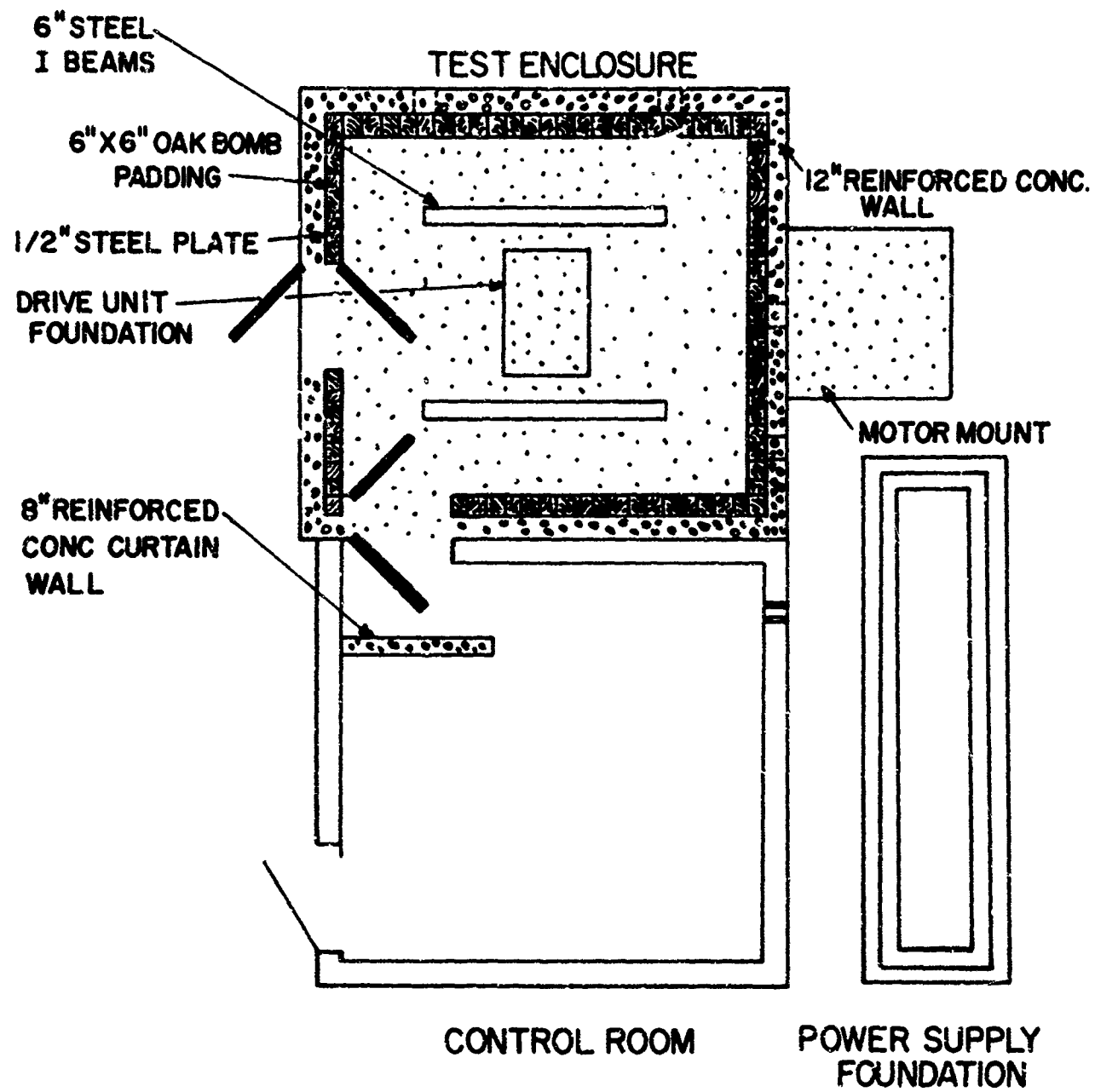


Figure 21. Physical Plant Layout

SECTION IX

INSTRUMENTATION AND DESIGN

1. Rotating Arm and Drive System Control

Control Console (Figure 22)

The rotating arm and drive system is operated and controlled from a remote operation console. The control panel includes a Start/Stop pushbutton with indicating light, a digital voltmeter for speed indication with a range of 0-4000 rpm with an accuracy of ± 10 rpm at maximum speed, a ten turn helipot enables speed set point resolution within 1% (manual adjusting to set speed as desired), and an emergency stop pushbutton with reset pushbutton to cut power to drive motor. Contained also, in the control panel are: D C voltmeter and ammeter, oil pressure and temperature visual indicators, an oil overtemperature relay with indicating light and an oil temperature regulator controlled manually by operator.

The characteristics of the individual components of the power train are shown in tabular form below:

Static Power Supply (Figure 23)

H. P.	400
Voltage Input	480 AC
Phase	3
Cycle	60
Operation	480-240 V, D. C.
One Minute Current	150%
Speed Regulation from No Load to Full Load	1%

Overload Protection **Thermal and Instantaneous Short Circuit Surge Protection**

Field Excitation 240 V, D.C.

Motor, Electric, DC

H. P.	400
RPM	(875-1750)
Voltage Input	Stabilized 480 DC
Insulation	Class B
Temperature Rise	60°C
Duty	Continuous
Windings	Shunt Wound
Mounting	Foot Mounted
Shaft	Ball Bearing, Horizontal
Enclosure	Open, Drip-proof
One Minute Current	150%
Operation	Adjustable 480-240 V, DC
Torque	Constant

Connecting Shaft

Length	80 1/2"
Power Transmission H. P.	400
Duty	Continuous
Safety Factor	1.5
Couplings (either end)	Matched

Speed Increasing Gear Set - Right Angle (Figure 24)

Ratio	(2:1)
Class	AGMA Class 1
Safety Factor	1.5
Output Shaft	Vertical
Input Shaft	Horizontal

Power Transmission H. P.	400
Load Limit for 1 Minute	150%
Lubrication	Motor Driven Oil Lube System
Oil Temperature Control	Manual
Indicators	Visual Temperature Indicator Visual Pressure Indicator

Hub and Drive Shaft (Figure 25)

Length	29 1/2"
Hub Diameter	17"
Material	4130 Steel
Duty	Continuous
Maximum Side Load	15,000 lb.

Bearings and Bearing Housing (Figure 26)

Type	Double Row Angular Contact
Duty	Medium
Radial Load Rating at 33 1/3 rpm	47,000 lb.
Average Life	2500 hrs.
Housing Material	Aluminum
Length	15 7/8"
Diameter	9 1/2"

Shaft and Bearing Housing Support Assembly (Figure 27)

Height	5' 4 1/2"
--------	-----------

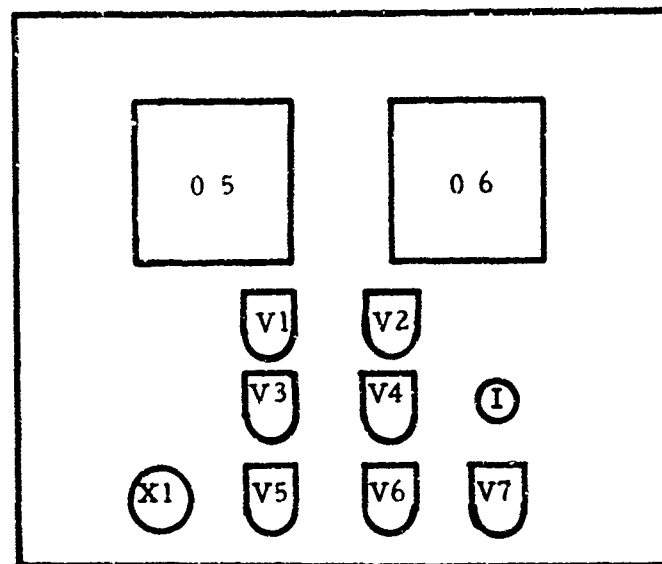


Figure 22. MOTOR DRIVE CONTROL PANEL

- | | |
|------------------------------|---------------------|
| V1 Oil Pressure Indicator | 05 D. C. Volt Meter |
| V2 Oil Temperature Indicator | 06 D. C. Ammeter |
| V3 Start Button | X1 Speed Control |
| V4 Stop Button | I Interlock |
| V5 Reset Button | |
| V6 A. C. Supply Button | |
| V7 Emergency Stop | |

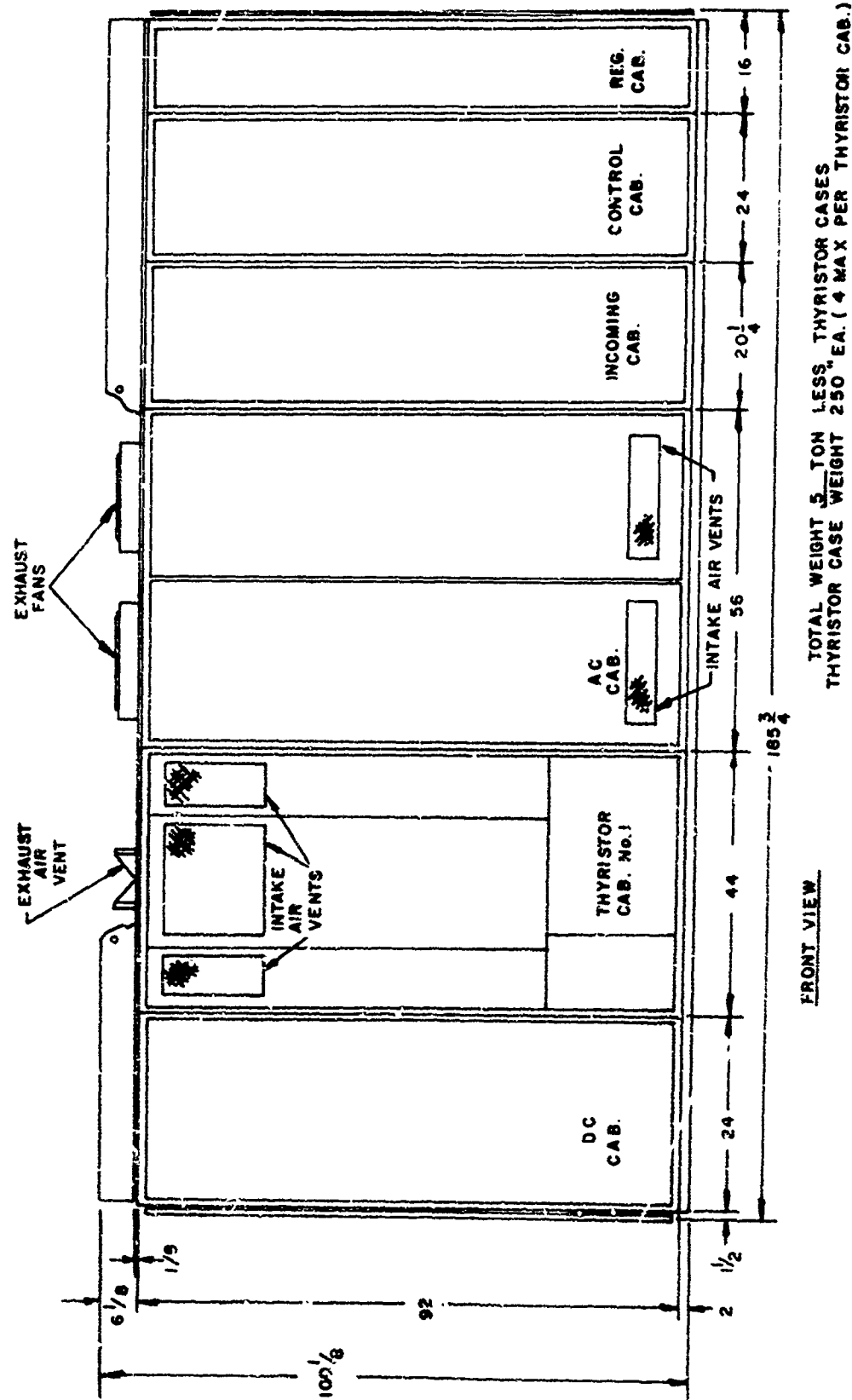


Figure 23. Static Power Supply

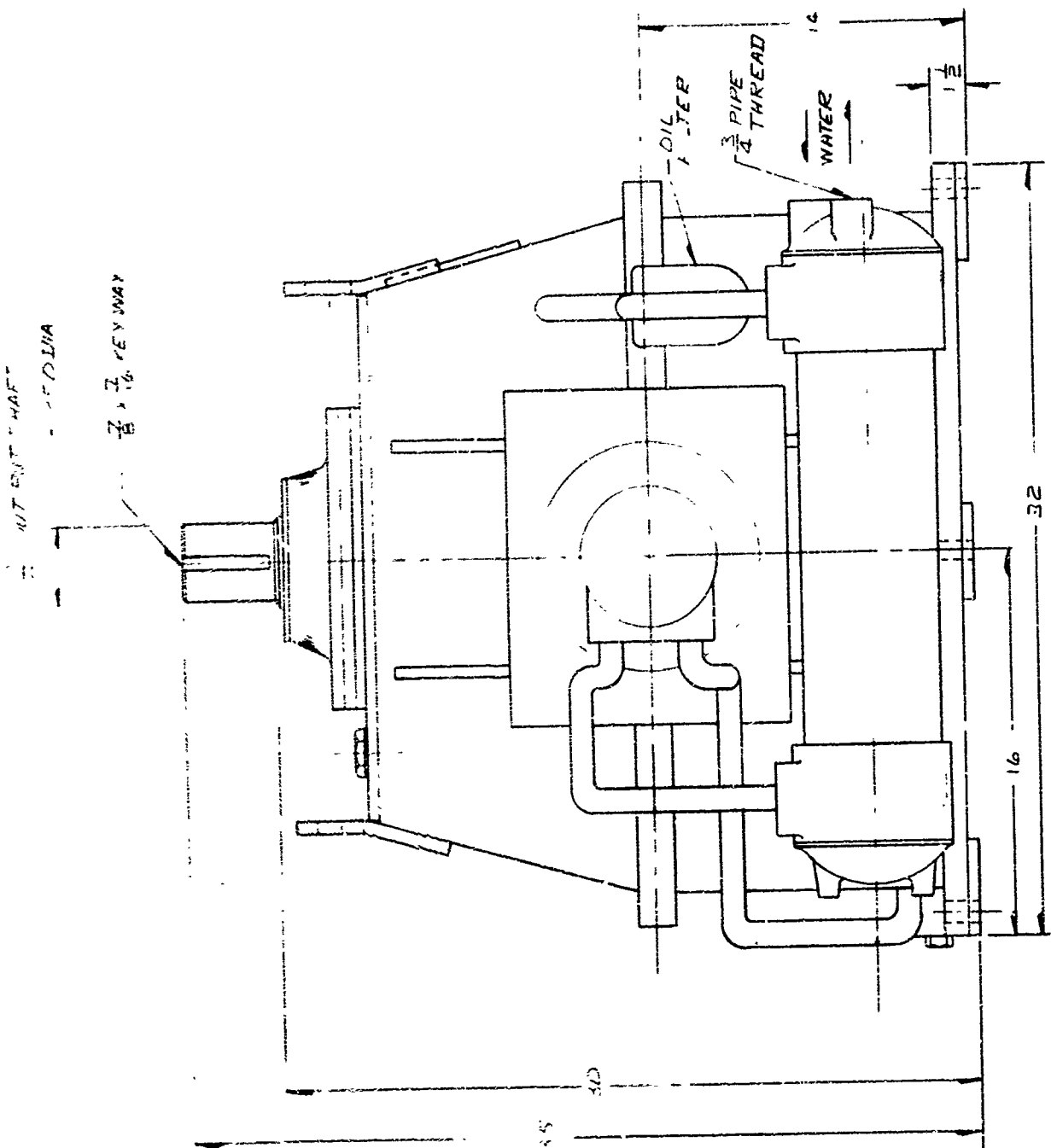


Figure 24. Speed Increasing Gear Set

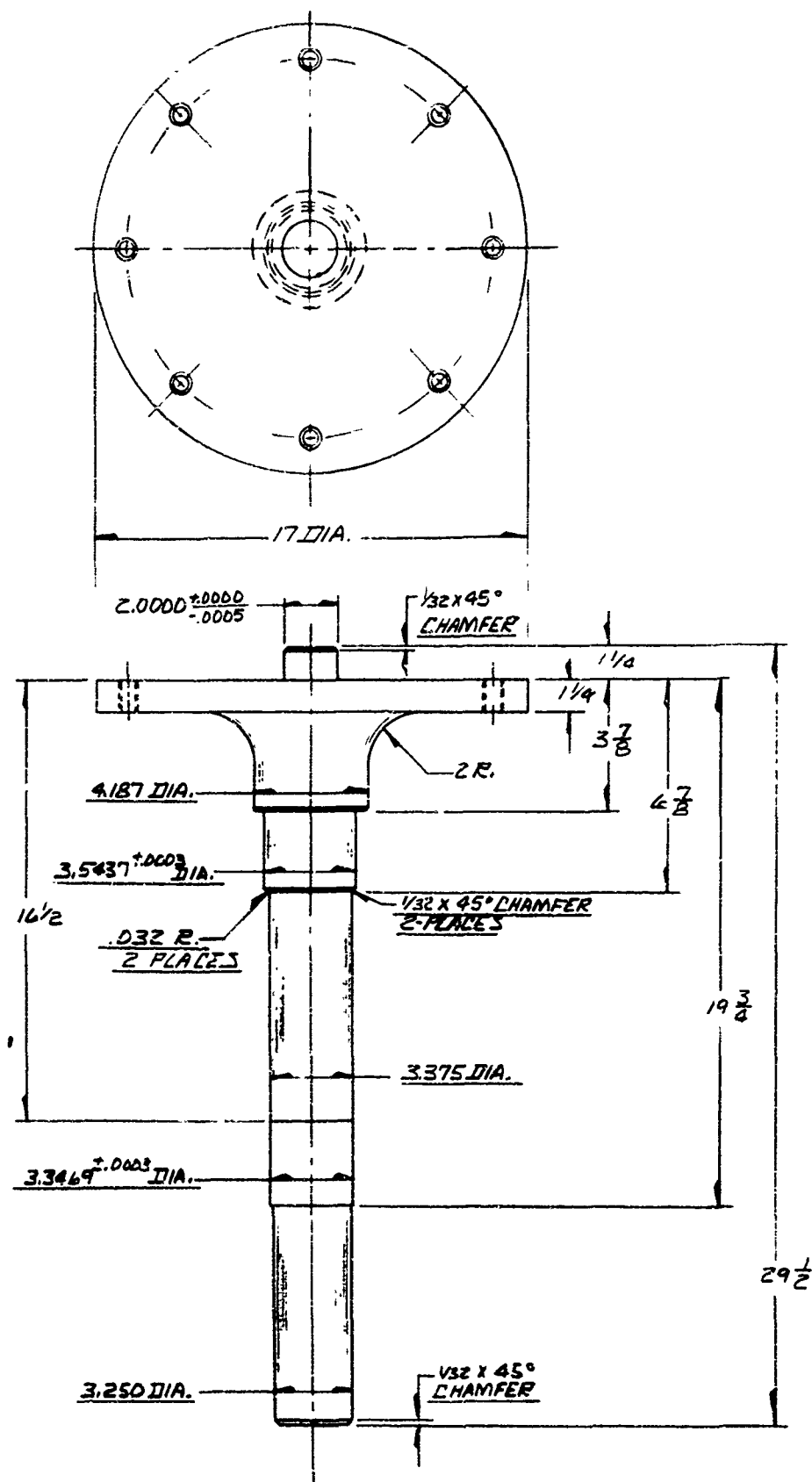


Figure 25. Hub and Drive Shaft

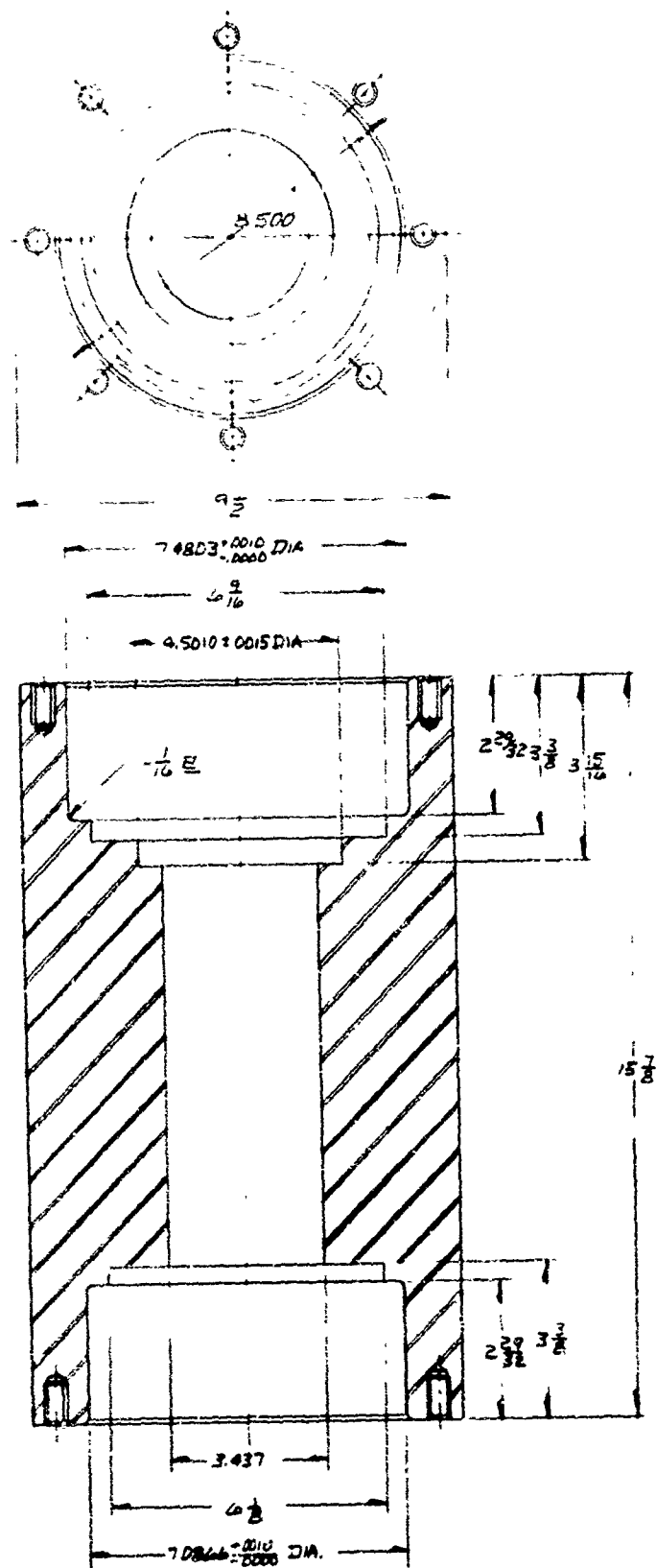
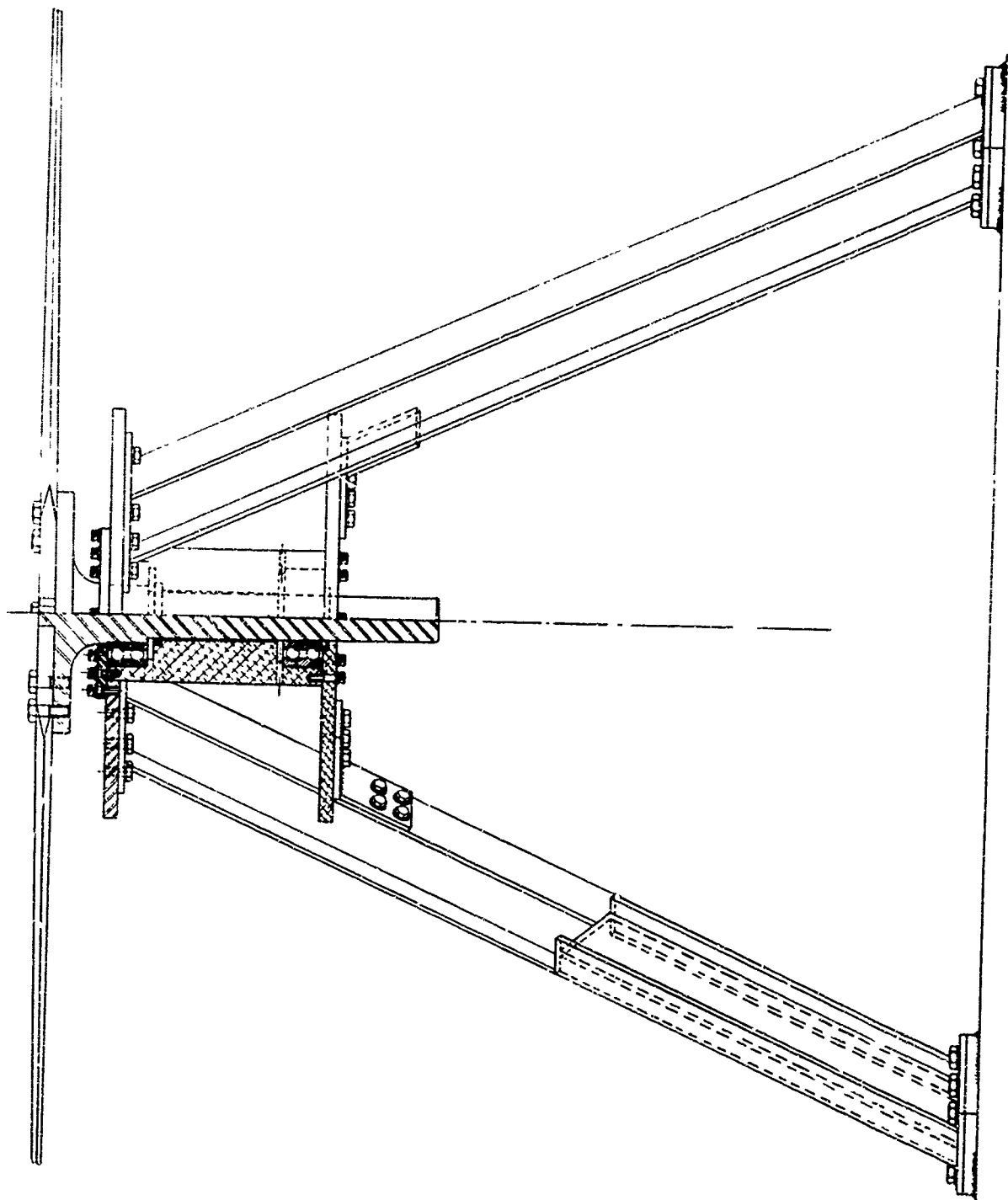


Figure 26. Bearing and Bearing Housing

Figure 27. Share and Bearing Housing Support Assembly



2. Rain Simulation Control

Control of the Simulated rainfall is accomplished at a remote control panel. When the test specimens have reached the desired velocity, the simulated rainfall is initiated. Start and stop switches open or close the solenoid valves located behind each of the four manifold quadrants. Rainfall is generated immediately and continues until termination of the test run. Clocking mechanisms provide a measurement of the total elapsed time of the rainfall during each test. Another clock mechanism provides a cumulative measurement of the total hours of rainfall simulation. A third clock measures total hours of rig operation.

At the termination of the operating day, a dumping solenoid is activated. This solenoid drains the water supply from the system. After the dumping solenoid is closed, nitrogen gas is forced through the quadrant solenoids, quadrants and capillary tubes to remove the remaining water.

The primary requirement in the generation of a simulated rainfall for use in rain erosion testing was that the mean drop size be 2.0 mm in diameter. An additional requirement was that it be possible to control the rainfall rate at values of 1 or 2 inches per hour in the path circumscribed by the test specimens. The system was designed for use with 96 capillaries operating simultaneously. Thus, the basic requirement for a 1 inch/hour rainfall required a 2.0 mm drop size falling at the rate of 6-7 drops/sec/capillary across two inches of the sample width.

It was found that a 27 gage (0.20 mm, I. D.) capillary, would produce a 2.0 mm drop at the rate of 6-7 drops/sec with a water head of approximately

5 ft. When the rainfall manifold quadrants with one hundred 27 ga capillaries were installed approximately 40 inches above the test specimens, they produced a simulated rainfall of 1 inch/hour across two inches of the specimen width. In actual practice, it was necessary to move the quadrants about 2 inches inboard of the specimen center for the outward pull of the drops due to centrifugal pumping of air created by the rotating arm. This outward pull was observed visually with binoculars from a position above the spaced bomb padding on the roof.

3. Closed Circuit Television Monitor and Camera

Test specimens are observed by a remote operator through a closed circuit television system. The television camera is enclosed in a blastproof environmental housing (See Figure 28). The interior walls of the housing are lined with styrofoam for sound proofing and noise adsorption. This is necessary due to the high noise level generated by the double rotating arm. The housing is mounted on the wall of the test enclosure above the plane of the blade. The camera lens is focused to a specific location in the annular path of the test specimen. Operator viewing is accomplished by an industrial display monitor in the remote control room. (See Figure 29). Illumination of the test specimens is obtained by a stroboscopic system synchronized to the rotation of the double arm. The enclosure wall directly in front of the television camera was painted white to provide an improved background contrast. The camera lens magnifies the test specimen image approximately 2.5 times actual size.

SPECIFICATIONS:	<u>Television Camera</u>	
	Input Voltage	125 volts AC
	Scanning	525 lines/frame; 30 frames/sec.
	Camera Tube Type	7735A vidicon
	Resolution	650 lines center; 450 lines corners
	Resolution Stability vs. Temperature	Stable (0° to 50°C)
	Scan Failure Protection	Less than 8 milliseconds
	Ambient Temperature Limits	0° to 50°C at 95% RH
	<u>Television Monitor</u>	
	Input Power	125 volts AC
	Video Signal	0.25 volt
	Video Response	800 line resolution

4. Vibration Monitor

Vibration pickups are mounted on the bearing housing below the double rotating arm. These seismic instruments measure displacement in the horizontal and vertical directions. The selected sensors operate in the 5 to 2000 cps frequency range with an accuracy of $\pm 2\%$, at 100 cps. Stable operation is possible between -65°F to 250°F. The vibration pickups serve various purposes such as indicating bearing conditions, shaft displacement, and unbalanced loading of the double rotating arm. A vibration measuring meter is located in the remote control room and provides direct readings of displacement in inches total amplitude. During normal operation of the rotating apparatus, vibration, displacement and/or unbalanced loading is constantly monitored.

Vibration Pickup

Frequency Range	5 to 200 cps
Sensitivity	650 ohms
Calibration Accuracy	$\pm 2\%$ at 100 cps
Temperature Range	-65° to 250°F

Vibration Meter

Scale Range	.001 to 1 inch total displacement
Tolerance	$\pm 2\%$
Frequency Range	10 to 1000 cps

TELEVISION CAMERA
③
ENVIRONMENTAL PROTECTIVE HOUSING

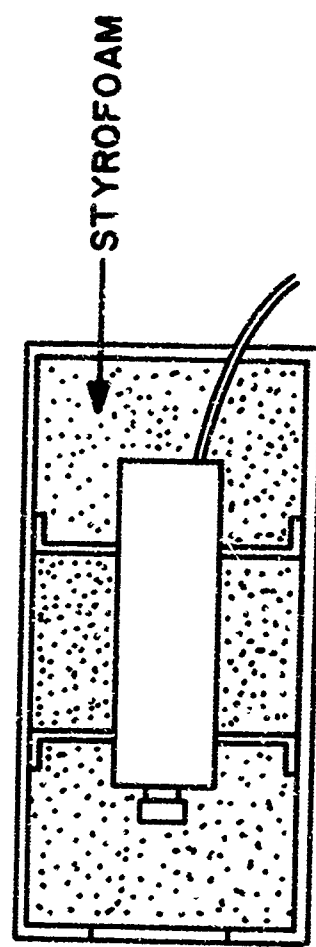


Figure 28. T. V. Camera and Environmental Housing

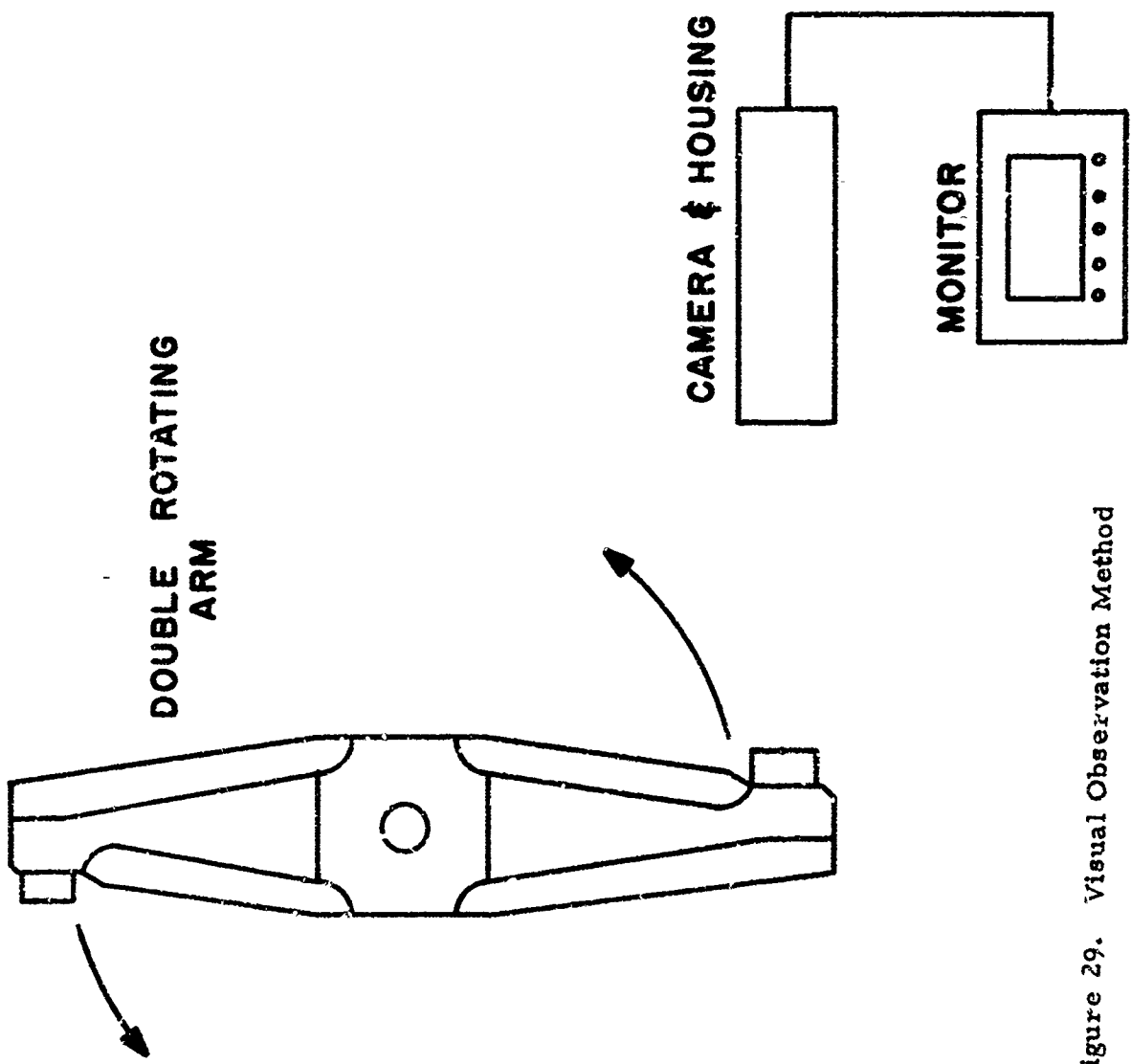


Figure 29. Visual Observation Method

5. Bearing Temperature Monitors

Temperature monitors are used to indicate the temperature of the axial and load bearings located on the rotating arm drive shaft. Two thermocouples 130° apart on the drive shaft bearing housing were placed at each bearing location. These temperature monitors are connected to a multipoint potentiometer recorder located in the remote control room. Constant and early warning are provided as to the axial and load bearings operational condition.

6. Stroboscopic System

In an effort to view the test specimens in the dynamic condition, a stroboscopic system was installed. The remote operator can determine specimen condition by the use of stroboscopy in conjunction with closed circuit television monitoring. A commercially available stroboscopic system was procured. With minor modification, the system is totally compatible with the television camera and monitor with respect to the necessary object illumination level and scanning rate of the camera. In essence, two high intensity stroboscopic lamps are mounted on the wall of the test enclosure, one above and one below the plane of the rotating double arm. The lamps are aligned, such that the intersection of their beams is in the area where the rotating test specimen is within the focal point of maximum clarity with respect to the television camera. The stroboscopic flash is triggered by photoelectric pickups located near the mounting shaft of the rotating double arm. The pickups respond to small reflective tapes mounted on the coupling of the rotating shaft. The location of the photoelectric pickups and reflective tapes are determined by the desired location of the test specimens with re-

spect to the television camera.

Two test specimens are evaluated simultaneously. They are located approximately 92.50 inches apart on the horizontal axis of the rotating double arm and in a rotational sense 180° apart. Therefore, in order to insure observation of either test specimen at the operator's discretion, the auto-synchronized stroboscope was modified to include an additional photoelectric pickup and switching arrangement. Selective monitoring of either test specimen is controlled by the operator. The stroboscopic equipment includes a control for a normal or bright illumination condition. This increases the operator observation capability regardless of the specimens' physical condition (light, dark, shiny, dull). (See Figure 30).

SPECIFICATIONS:

Flash Rate

Normal Setting	0-12,000/min
Bright Setting	0-5,000/min

Flash Duration

8 Microsec/max.

Flash Tube (Xenon)

15° beam
50,000,000 flashes

Photo Pickup

Speed range	0 to 500,000 events/min
Resolution	Senses 0.01" line
Photo Cell	Silicon
Life Expectancy	100,000 hours

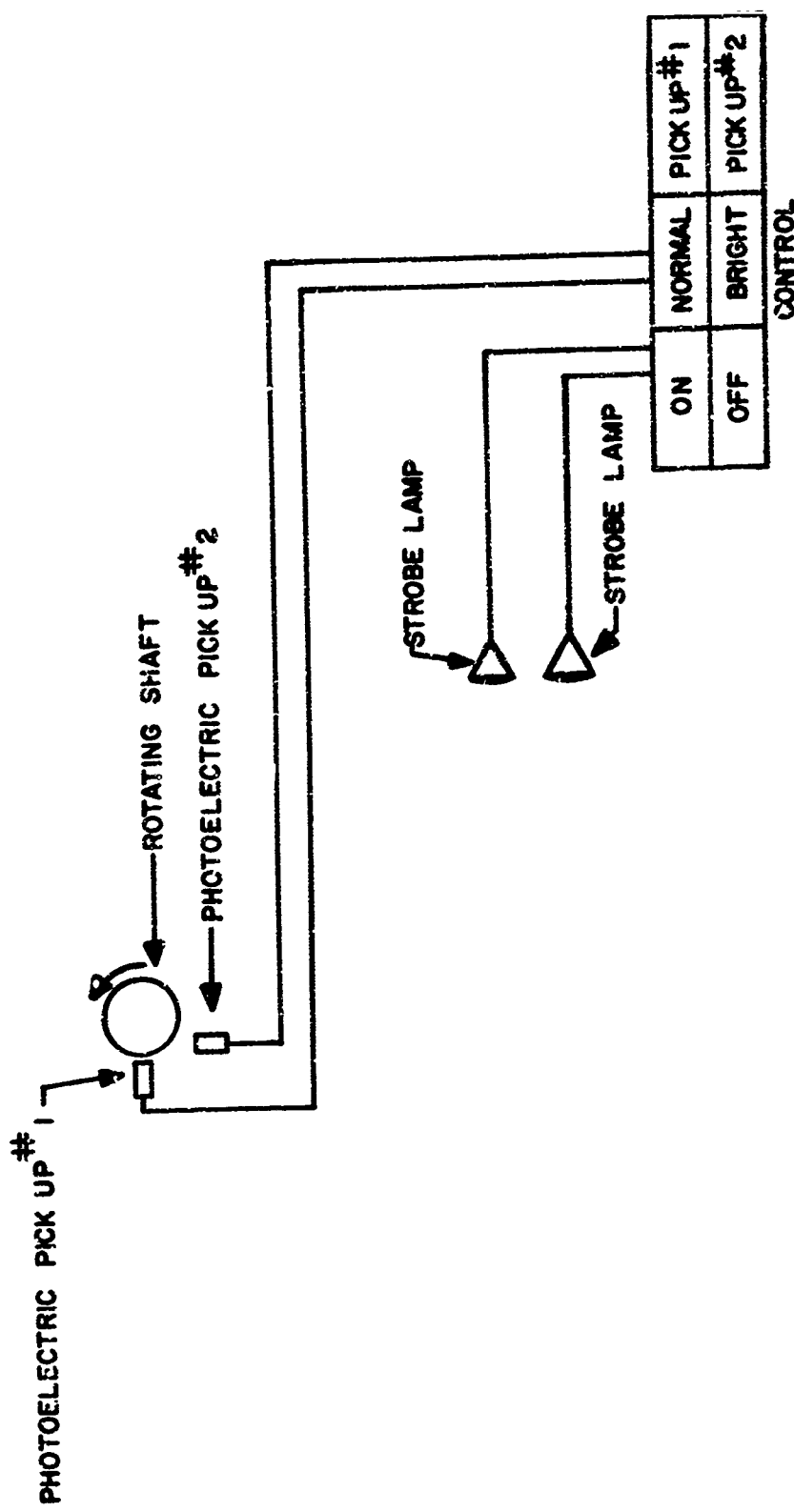


Figure 30. Stroboscopic System

SECTION X

CALIBRATION EXPERIMENTS

The initial characterization of the rainfall patterns and behavior of the apparatus was measured by the use of uncoated glass-epoxy laminate airfoils which indicated the erosion pattern on their leading edge surface. The patterns proved to be quite uniform and so weight loss experiments on 1100 aluminum were conducted to check reproducibility. The weight loss was reproducible within 5 milligrams of total of 150 mg eroded after runs of 20 minutes at 600 MPH in the 1 inch/hour simulated rainfall.

Following the above experiments, a large number of aluminum and glass-epoxy airfoils coated with two thicknesses (8 and 12 mils) of each of the neoprenes qualified to MIL-C-7439B Types I and II and MIL-C-27315 Type I Specifications were run at 500 MPH to measure their erosion resistance. This was determined as the time for penetration to the substrate or for adhesion loss of the coating as observed through the closed circuit television viewing system.

The results were as expected with the coatings lasting longer on the aluminum substrates than on the glass-epoxy laminate. This reflects the substrate dependence of the coating. The thickness dependence of the erosion resistance of elastomeric coatings was also demonstrated in these neoprene coatings with considerable differences in the times to failure for 8 mils (typically 10-15 minutes at 500 MPH on aluminum) versus 12 mils (typically 25-40 minutes at 500 MPH on aluminum).

The specific data on these neoprene-coated specimens is shown in Table VI.

TABLE VI
RAIN EROSION DATA
500 MPH, 1 inch/hour Simulated Rainfall (1.8 mm dia drops)

Specimen No.	Coating	Coating Thickness (mils)	Substrate	Failure Time (min)	Remarks (type of failure, etc.)
A-23-56-8-1	MIL-C-7439B Neoprene Type I	8	aluminum	18.3	erosion failure, immediate
A-23-56-8-2	"	8	"	18.3	slight surface erosion
A-23-56-8-3	"	8	"	19.9	slight surface erosion
A-23-56-8-4	"	8	"	19.9	erosion failure, immediate
A-23-56-12-1	"	12	"	15.5	slight surface erosion
A-23-56-12-2	"	12	"	15.5	erosion failure, inboard
A-23-56-12-3	"	12	"	22.4	slight surface erosion
A-23-56-12-4	"	12	"	22.4	erosion failure
A-23-56-12-5	"	12	"	41.6	surface dulling and roughening
A-23-56-12-6	"	12	"	41.6	erosion failure
E-23-57-8-1	MIL-C-7439B Neoprene Type II	8	glass-epoxy	42.5	tape failure twice
E-23-57-8-2	"	8	"	42.5	tape failure twice, one sample erosion
E-23-57-8-3	"	8	"	10.8	severe surface erosion and some pitting
E-23-57-8-4	"	8	"	10.8	erosion failure
E-23-57-12-1	"	12	"	35.0	erosion failure
E-23-57-12-2	"	12	"	25.0	erosion failure
E-23-57-12-3	"	12	"	51.4	severe surface erosion and some pitting
E-23-57-12-4	"	12	"	51.4	erosion failure
E-N-79-8-1	MIL-C-7439B Neoprene Type I	8	"	15.1	erosion failure
E-N-79-8-2	"	8	"	15.1	erosion failure
E-N-79-8-3	"	8	"	10.1	erosion failure

TABLE VI (cont'd)
 RAIN EROSION DATA
 500 MPH, 1 inch/hour Simulated Rainfall (1.8 mm dia drops)

Specimen No.	Coating	Coating Thickness (mils)	Substrate	Failure Time (min)	Remarks (type of failure, etc)
E-N-79-8-4	MIL-C-7439B Neoprene Type I	8	glass-epoxy	10.1	erosion failure
E-N-79-12-1	"	"	"	29.4	erosion failure
E-N-79-12-2	"	"	"	19.4	severe sample erosion
E-N-79-12-3	"	"	"	19.2	erosion failure
E-N-79-12-4	"	"	"	19.2	moderate sample erosion
A-N-810-8-1	MIL-C-7439B Neoprene Type II	8	aluminum	10.0	coating failure tore from side
A-N-810-8-2	"	"	"	10.0	slight surface erosion
A-N-810-8-3	"	"	"	19.9	slight surface erosion
A-N-810-8-4	"	"	"	19.9	erosion failure
A-N-810-12-1	"	"	"	3.5	very slight surface erosion
A-N-810-12-2	"	"	"	3.5	erosion or defect failure
A-N-810-12-3	"	"	"	7.7	coating tore from back forward
A-N-810-12-4	"	"	"	7.7	very slight surface erosion
A-N-83-12-1	MIL-C-27315 Neoprene Type I	12	"	0.8	sample tore from substrate
A-N-83-12-2	"	"	"	0.8	O.K.
A-N-83-12-3	"	"	"	1.9	adhesion failure at
A-N-83-12-4	"	"	"	0.2 min	0.2 min
E-23-60-12-1	"	"	"	1.9	adhesion failure
			12	14.5	erosion failure
			glass-epoxy		

TABLE VI (cont'd)
 RAIN EROSION DATA
 500 MPH, 1 inch/hour Simulated Rainfall (1.8 mm dia drops)

Specimen No.	Coating	Thickness (mils)	Coating	Substrate	Failure Time (min)	Remarks (type of failure, etc)
E-23-60-12-2	MIL-C-27315 Neoprene Type I	12	glass-epoxy	"	22.8	piece tore from back at 19.2 eroded forward
E-23-60-12-3	"	"	12	"	22.8	moderate surface erosion
E-23-60-12-4	"	"	12	"	19.3	erosion failure
E-N-83-12-1	"	"	12	"	19.3	blistering with one small tear
E-N-83-12-2	"	"	12	"	14.5	erosion failure
E-N-83-12-3	"	"	12	"	24.6	erosion failure at 19.6 min., bottom
E-N-83-12-4	"	"	12	"	24.6	severe surface erosion
A-23-60-12-1	"	"	12	aluminum	18.4	moderate surface erosion
A-23-60-12-2	"	"	12	"	13.4	erosion failure
A-23-60-12-3	"	"	12	"	50.6	slight erosion OB edge
A-23-60-12-4	"	"	12	"	50.6	erosion failure OB edge
E-N-810-12-1	MIL-C-7439 Neoprene Type II	12	glass-epoxy	"	34.5	slight surface erosion and blistering
E-N-810-12-2	"	"	12	"	34.5	erosion failure
E-N-810-12-3	"	"	12	"	35.5	slight blistering
E-N-810-12-4	"	"	8	"	35.5	erosion failure OB
E-N-810-8-1	"	"	8	"	3.3	erosion failure, outboard O.K.
E-N-810-8-2	"	"	8	"	7.1	erosion failure OB edge
E-N-810-8-3	"	"	8	"	7.1	slight blistering OB
E-N-810-8-4	"	"	8	"	21.4	erosion failure
A-N-79-12-1	MIL-C-7439B Neoprene Type I	12	aluminum	"	21.4	slight erosion failure
A-N-79-12-2	"	"	12	"	21.4	slight roughing
A-N-79-12-3	"	"	"	"	22.1	

TABLE VI (cont'd)

RAIN EROSION DATA
500 MPH, 1 inch/hour Simulated Rainfall (1.8 mm dia drops)

Specimen No.	Coating	Coating Thickness (mils)	Substrate	Failure Time (min)	Remarks (type of failure, etc)
A-N-79-8-4	MIL-C-7439B Neoprene Type I	8	aluminum	0.6	O. K.
A-23-57-12-1	MIL-C-7439B Neoprene Type II	12	"	35.0	
A-23-57-12-2	"	12	"	35.0	started to erode at 31.2 approx 1/2" from outboard
A-23-57-12-3	"	12	"	86.8	slight erosion
A-23-57-12-4	"	12	"	86.8	erosion failure
A-23-57-8-1	"	8	"	18.8	erosion, bottom OB top IB
A-23-57-8-2	"	8	"	18.8	no erosion
A-23-57-8-3	"	8	"	17.5	O. K.
A-23-57-8-4	"	8	"	17.5	erosion failure
E-23-56-12-1	MIL-C-7439B Neoprene Type I	12	glass~ epoxy	29.0	erosion failure
E-23-56-12-2	"	12	"	29.0	slight blistering
E-23-56-12-3	"	12	"	5.4	O. K.
E-23-56-12-4	"	12	"	5.4	rough surface before run tore coating
E-23-56-12-5	"	12	"	12.2	no failure
E-23-56-12-6	"	12	"	12.2	erosion failure
E-23-56-8-1	"	8	"	6.6	slight surface erosion
E-23-56-8-2	"	8	"	6.6	erosion failure
E-23-56-8-3	"	8	"	--	substrate too large, did not run
E-23-56-8-4	"	8	"	--	substrate too large, did not run

SECTION XI

CORRELATION EXPERIMENTS

The old AFML rotating arm (500 mph only) apparatus had been previously correlated with the flight test results from the Project Rough Rider thunder-storm penetration flights in 1967. (Reference 1). The same materials were also run in the new apparatus at 500 mph, 1 inch/hour simulated rainfall. Specimens of the various coatings were prepared utilizing aluminum substrates which are representative of the horizontal stabilizer leading edge of the F-100 F aircraft.

The results of these experiments are shown in Table VII which compares the time to failure in the new apparatus with the time for failure after a measured time in the thunderstorms on the aircraft. As may be seen, the rankings of the materials agree quite well with the exception of the clear 23-61 polyurethane which performed relatively better in the flight test than it did in the rotating arm exposure. The modes of failure-erosion or adhesion loss -- were also similar for most materials in either the rotating arm or flight exposure.

TABLE VII
COMPARISON OF ROTATING ARM EROSION
AND FLIGHT TEST EROSION

Material	Rotating Arm ¹ Time to Failure (minutes)	Type of Failure	Flight Test ² Time to Failure (minutes)	Type of Failure
Specification neoprene (0.015") MIL-C-7439B	46.0	Erosion	137:15	Erosion
Clear urethane (0.015") 23-61	9.8	Erosion	439:40 ³	Little erosion
White urethane (0.015") MS-61P	180.0	Slight erosion	439:40 ³	No erosion
Clear urethane (0.015") MS-61	180.0	No failure	439:40 ³ (391:55)	No erosion Adhesion
Electroplated nickel (0.015")	180.0	No damage	439:40 ³	No erosion
Y-9265 urethane tape (0.013")	3.0	Adhesion & erosion	137:15	Adhesion
Estane boot (0.018")	84.3	Adhesion	214:10	Adhesion
Neoprene boot (0.022")	117.0	Erosion	137:15	Erosion & adhesion
Nitrile rubber boot (0.018")	52.1	Erosion	137:15	Erosion & adhesion
P.O. 655 polyurethane sheet (0.030")	not run	Adhesion	338:10	Adhesion
Neoprene boot with gum rubber backing (0.039")	61.0	Adhesion	184:10	Adhesion
White neoprene (0.022")	87.6	Erosion	61:55	Adhesion

¹ Rotating arm exposure - 500 mph, 1 inch/hour rainfall intensity in AFML Mach 1.2 apparatus.

² Flight test exposure - 300 mph, varying intensities of rain and hail.

³ Full exposure on F-100 F aircraft.

NOTES: All coatings and boots are identical thicknesses on aircraft and rotating arm specimens. Substrates are aluminum. 180 minutes is normal cut-off time for specimens on AFML apparatus.

SECTION XII

DISCUSSION OF RESULTS

The experimentation with the apparatus at 500 and 600 MPH to date have indicated all components are functioning as planned and the degree of simulation provided by this rotating arm is much improved over previous such apparatus. The consistency and reproducibility of the results are excellent.

The individual subsystems including the power supply and drive system, the rotating arm, the water supply and droplet simulation apparatus, the stroboscopic system, closed circuit television, and monitoring systems, the vibration and temperature sensing system and the safety features combine to provide one of the most sophisticated rain erosion simulation devices currently in operation. Over 700 operating hours have been completed, representing more than 850 test runs. More than 1600 specimens have been tested and evaluated at 500 and 600 MPH.

Initial rotating arm results and correlation of these results with actual flight test results indicate a capability exists not only for simulation of the rain erosion phenomena and mechanisms on varying materials but more importantly for use in development of improved rain erosion resistant materials.

SECTION XIII

CONCLUSIONS

1. A rotating arm apparatus has been constructed at the Air Force Materials Laboratory, Wright-Patterson AFB, Ohio, which is capable of rain erosion simulation at velocities up to 900 MPH.
2. The apparatus has demonstrated consistency and reproducibility in its operation.
3. The rankings of the rain erosion resistance of materials as obtained on this rotating arm have correlated with those obtained in actual flight exposures.
4. The rotating arm method is the most effective research tool for guiding exploratory development of rain erosion resistant materials.

SECTION XIV

FUTURE WORK

1. Research on the rotating arm apparatus will continue to investigate the erosion behavior of new and improved elastomeric, plastic, ceramic and metallic coatings and bulk materials at velocities up to Mach 1.2.
2. High speed motion picture photography will be utilized to develop models of mechanisms of erosion of ductile, brittle and composite materials.
3. Effects of environmental variables such as velocity, impingement angle, droplet size and rainfall concentration will be investigated.
4. Effects of materials variables such as coating thickness, composite, construction techniques, void content and fiber or matrix composition will be investigated.

SECTION XV
REFERENCES

1. G. F. Schmitt, Jr., Research for Improved Subsonic and Supersonic Rain Erosion Resistant Materials, AFML-TR-67-211, January 1968.
2. G. F. Schmitt, Jr., Flight Test-Whirling Arm Correlation of Rain Erosion Resistance of Materials, AFML-TR-67-420, September 1968.
3. N. E. Wahl, Investigation of the Phenomena of Rain Erosion at Subsonic and Supersonic Speeds, AFML-TR-65-330, October 1965.
4. J. Beal and N. E. Wahl, Study and Design of Supersonic Rotating Arm Test Apparatus, WADC-TR-57-435, July 1957.

UNCLASSIFIED

Security Classification

DOCUMENT CONTROL DATA - R & D

(Security classification of title, body of abstract and indexing annotation must be entered when the overall report is classified)

1. ORIGINATING ACTIVITY (Corporate author) Air Force Materials Laboratory Wright-Patterson AFB Ohio 45433		2a. REPORT SECURITY CLASSIFICATION UNCLASSIFIED 2b. GROUP NONE
3. REPORT TITLE "Development and Calibration of a Mach 1.2 Rain Erosion Test Apparatus"		
4. DESCRIPTIVE NOTES (Type of report and inclusive dates) March 1966 to August 1969		
5. AUTHOR(S) (First name, middle initial, last name) Charles J. Hurley George F. Schmitt, Jr.		
6. REPORT DATE October 1970	7a. TOTAL NO. OF PAGES 68	7b. NO. OF REFS 4
8a. CONTRACT OR GRANT NO.	8b. ORIGINATOR'S REPORT NUMBER(S) AFML-TR-70-240	
b. PROJECT NO. 7340	9b. OTHER REPORT NO(S) (Any other numbers that may be assigned this report)	
c. Task No. 734007		
d.		
10. DISTRIBUTION STATEMENT This document has been approved for public release and sale; its distribution is unlimited.		
11. SUPPLEMENTARY NOTES	12. SPONSORING MILITARY ACTIVITY Air Force Materials Laboratory Air Force Systems Command Wright-Patterson AFB Ohio 45433	
13. ABSTRACT Development of a Mach 1.2 Rain Erosion Test Apparatus at the Air Force Materials Laboratory, Wright-Patterson Air Force Base, Ohio, is described. This rotating arm apparatus is capable of evaluating the relative rain erosion resistance of materials and can be operated at speeds of 450 to 900 mph in a 1 or 2 inch/hour simulated rainfall. This report describes the design and development of the apparatus including the rotating arm, power train, test enclosure, rain simulation and control systems. Calibration and correlation experiments are also described.		
Distribution of this abstract is unlimited.		

DD FORM 1 NOV 65 1473

UNCLASSIFIED
Security Classification

UNCLASSIFIED

Security Classification

14 KEY WORDS	LINK A		LINK B		LINK C	
	ROLE	WT	ROLE	WT	ROLE	WT
Rain Erosion Rotating Arm Apparatus						

UNCLASSIFIED

Security Classification